Linkage Dependent Charge Separation and Charge Recombination in Porphyrin-Pyromellitimide-Fullerene Triads

Hiroshi Imahori,*,† Koichi Tamaki,‡ Yasuyuki Araki,§ Taku Hasobe,|| Osamu Ito,*,§ Akihisa Shimomura,⊥ Santi Kundu,⊥ Tadashi Okada,*,⊥ Yoshiteru Sakata,‡ and Shunichi Fukuzumi*,||

Department of Material and Life Science, Graduate School of Engineering, Osaka University, CREST, Japan Science and Technology Corporation (JST), Suita, Osaka 565-0871, Japan, and The Institute of Scientific and Industrial Research, Osaka University, 8-1 Mihoga-oka, Ibaraki, Osaka 567-0047, Japan, and Institute for Multidisciplinary Research for Advanced Materials, Tohoku University, CREST, Japan Science and Technology Corporation (JST), Katahira, Aoba-ku, Sendai 980-8577, Japan, and Department of Chemistry, Graduate School of Engineering Science and Research Center for Materials Science at Extreme Conditions, Osaka University, Toyonaka, Osaka 560-0043, Japan

Received: December 5, 2001

A homologous series of zincporphyrin (ZnP)-pyromellitimide (Im)-C_{60} linked triads where the pyromellitimide (Im) moiety is incorporated as an intermediate acceptor between the above two chromophores with a linkage of different spacers, **ZnP-Im-CH$_2$-C$_{60}$**, **ZnP-Im-C$_{60}$**, and **ZnP-CH$_2$-Im-C$_{60}$** as well as the reference dyads (**ZnP-Im-CH$_2$-ref**, **ZnP-Im-ref**, and **ZnP-CH$_2$-Im-ref**) have been prepared to investigate linkage dependence of photoinduced electron transfer (ET) and back ET to the ground state in the triads. Time-resolved transient absorption spectra of the triads measured by picosecond laser photolysis as well as the fluorescence lifetimes in THF reveal the occurrence of photoinduced ET from the singlet excited state of the ZnP to the Im moiety to give the initial charge-separated state, i.e., the zincporphyrin radical cation ($ZnP^{\bullet+}$)-imide radical anion ($Im^{\bullet-}$) pair, followed by a charge shift (CSH) to produce the final charge-separated state, the $ZnP^{\bullet+}$-$C_{60}^{\bullet-}$ pair. The rate constants of photoinduced ETs in **ZnP-Im-C$_{60}$** (1.8×10^{10} s^{-1}) and **ZnP-Im-CH$_2$-C$_{60}$** (1.3×10^{10} s^{-1}) in THF are much larger than those in **ZnP-CH$_2$-Im-C$_{60}$** (2.9×10^{9} s^{-1}) and **ZnP-CH$_2$-Im-ref** (1.9×10^{9} s^{-1}). The larger charge separation (CS) rates in the former case are ascribed to the relatively strong electronic coupling because of the absence of a methylene linkage between the ZnP and the Im moieties in **ZnP-Im-C$_{60}$** and **ZnP-Im-CH$_2$-C$_{60}$** as compared to the triad and dyad with the methylene linkage. The transient absorption spectra of the final charge-separated state, the $ZnP^{\bullet+}$-$C_{60}^{\bullet-}$ pair, have been also measured by nanosecond laser photolysis. It has been found that the rate constants of charge recombination (CR) of **ZnP$^{\bullet+}$-Im-C$_{60}^{\bullet-}$** are temperature independent, but that the CR rate constants of **ZnP$^{\bullet+}$-Im-CH$_2$-C$_{60}^{\bullet-}$** exhibit an Arrhenius-like temperature dependence with an activation energy of 0.13 eV which corresponds to the energy difference between **ZnP$^{\bullet+}$-Im$^{\bullet-}$-CH$_2$-C$_{60}$** and **ZnP$^{\bullet+}$-Im-CH$_2$-C$_{60}^{\bullet-}$**. This indicates that the relatively strong electronic coupling without methylene linkage in **ZnP-Im-C$_{60}$** results in the preference of the tunneling superexchange ET over the sequential ET in the CR process which requires the thermal activation to reach the higher energy state (i.e., **ZnP$^{\bullet+}$-Im$^{\bullet-}$-C$_{60}$**), whereas the sequential ET predominates in the triads with the methylene linkage.

Introduction

There has been considerable interest and discussion about the relative importance of a direct superexchange (coherent) process in electron transfer (ET) between electron donors (D) and acceptors (A) linked by bridges (B) in D−B−A systems (in which $D^{\bullet+}-B^{\bullet-}-A$ plays the role of a virtual state) versus a sequential (incoherent) process which involves a bona fide intermediate $D^{\bullet+}-B^{\bullet-}-A$.[1−3] Incoherent sequential ET dominates over coherent superexchange ET when ET from D to B as well as from B to A is exothermic, whereas the relative importance of sequential versus superexchange ET may be altered by a subtle change in the driving force and the electronic coupling in each ET step when ET from D to B is slightly endothermic or thermoneutral and ET from B to A is exothermic. Such an argument will be also applicable to charge recombination (CR) processes from $A^{\bullet-}$ to $D^{\bullet+}$. Namely, direct superexchange-mediated ET occurs from $A^{\bullet-}$ to $D^{\bullet+}$ or sequential ET takes place from $A^{\bullet-}$ to $D^{\bullet+}$ via $D^{\bullet+}-B^{\bullet-}-A$. However, a switch between sequential and superexchange ET, especially for CR processes, has yet to be fully studied in a homologous series of D−B−A systems.[2−14]

We report herein such a system to demonstrate a switch between sequential and superexchange ET using a homologous series of zincporphyrin (ZnP)-C_{60} linked triads where the pyromellitimide (Im) moiety is incorporated as an intermediate

* To whom correspondence should be addressed. E-mail: imahori@mee3.moleng.kyoto-u.ac.jp; ito@tagen.tohoku.ac.jp; okada@chem.es.osaka-u.ac.jp; fukuzumi@ap.chem.eng.osaka-u.ac.jp.

† Kyoto University.

‡ The Institute of Scientific and Industrial Research, Osaka University.

§ Tohoku University.

|| Graduate School of Engineering, Osaka University.

⊥ Science and Research Center for Materials Science at Extreme Conditions, Osaka University.

10.1021/jp014433f CCC: $22.00
Published on Web 03/05/2002

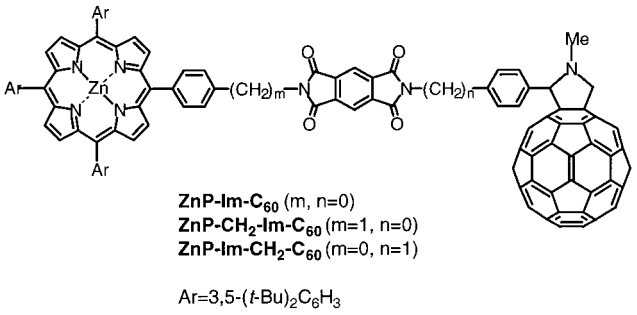

Figure 1. Porphyrin-pyromellitimide-C_{60} triads.

acceptor between the above two chromophores with a linkage of different spacers (**ZnP-Im-CH$_2$-C$_{60}$** ($m = 0$ and $n = 1$)), **ZnP-Im-C$_{60}$** (m and $n = 0$)[15] and **ZnP-CH$_2$-Im-C$_{60}$** ($m = 1$ and $n = 0$), as shown in Figure 1. The energy gradient of each state in ZnP-$(CH_2)_m$-Im-$(CH_2)_n$-C_{60} is well tuned to display sequential ET within a molecule (i.e., $^1ZnP^*$-$(CH_2)_m$-Im-$(CH_2)_n$-C_{60} → $ZnP^{\bullet+}$-$(CH_2)_m$-$Im^{\bullet-}$-$(CH_2)_n$-C_{60} → $ZnP^{\bullet+}$-$(CH_2)_m$-Im-$(CH_2)_n$-$C_{60}^{\bullet-}$). This type of sequential ET, which is similar to initial charge separation (CS) event in photosynthesis, has not been reported in donor-linked fullerenes.[15−27]

Because fullerenes exhibit small reorganization energies (λ) in ET,[23−28] photoinduced CS and CR are accelerated and decelerated, respectively, which have been observed frequently in donor-linked fullerenes.[23−27] Thus, the CR rates from the $C_{60}^{\bullet-}$ to the $ZnP^{\bullet+}$ in the resulting final charge-separated state of the present triads can be markedly slowed by shifting them deep into the inverted region of the Marcus parabola. Taking into account the fact that the first reduction potentials of the Im are more negative by ~0.1 V than those of the C_{60},[15] the CR processes will be affected greatly by the Im moiety as a "stepping stone". In this study, the effects of linkage on the CR processes as well as the CS processes in the triads are examined in detail by time-resolved transient absorption spectroscopy and fluorescence lifetime measurements.

Results and Discussion

Synthesis and Characterization. The synthetic routes to **ZnP-Im-CH$_2$-C$_{60}$**, **ZnP-Im-C$_{60}$**,[15] and **ZnP-CH$_2$-Im-C$_{60}$** are shown in Scheme 1. Cross-condensation of aminoporphyrin **1a**,[23b] pyromellitic dianhydride **2**, and formyl-protected benzylamine **3a**[29] or aniline **3b**,[30] followed by acid hydrolysis, gave pyromellitimide-substituted porphyrins **4a** and **4b** in 25 and 19% yield, respectively. Similar cross-condensation of aminomethylporphyrins **1b**, **2**, and **3b** and subsequent acid hydrolysis afforded pyromellitimide-substituted porphyrin **4c** in 13%. The zincporphyrin-pyromellitimide-C_{60} triads (**ZnP-Im-CH$_2$-C$_{60}$**, **ZnP-Im-C$_{60}$**, and **ZnP-CH$_2$-Im-C$_{60}$**) were obtained in 23−42% yield by 1,3-dipolar cycloadditions[31] with **4a**−**c**, C_{60}, and *N*-methylglycine in toluene and subsequent treatment with zinc acetate. Porphyrin-pyromellitimide dyads [**ZnP-Im-CH$_2$-ref** (m=0, n=1, R=CH_3), **ZnP-Im-ref** (m, n=0, R=$C_{16}H_{33}$), and **ZnP-CH$_2$-Im-ref** (m=1, n=0, R=$C_{16}H_{33}$)] as well as porphyrin and C_{60} references [**ZnP-ref**[23b] (m=0), **ZnP-CH$_2$-ref** (m=1), and **C$_{60}$-ref**[25a]] were also prepared (Figure 2). Structures of all new compounds were confirmed by spectroscopic analysis including ^{1}H NMR, IR, and FAB mass spectra (see the Experimental Section). The absorption spectra of **ZnP-Im-CH$_2$-C$_{60}$**, **ZnP-Im-C$_{60}$**, and **ZnP-CH$_2$-Im-C$_{60}$** in THF are virtually linear combinations of the absorption spectra of each chromophore, giving no indication for strong interactions between these chromophores in the ground state.

Similar results were obtained in 1,4-dioxane. The center-to-center distance (R_{cc}) and edge-to-edge distance (R_{ee}) were estimated by molecular mechanic calculations (MacroModel, version 6.0) and summarized in Table 1.

Photophysics of Porphyrin-Pyromellitimide Dyads. At first, the photodynamics of the dyad systems (**ZnP-Im-CH$_2$-ref**, **ZnP-Im-ref**, and **ZnP-CH$_2$-Im-ref**) were investigated for the better understanding of the more complex triad systems. Time-resolved transient absorption spectra of the dyads were measured by picosecond laser photolysis. Upon excitation of **ZnP-Im-CH$_2$-**

SCHEME 1

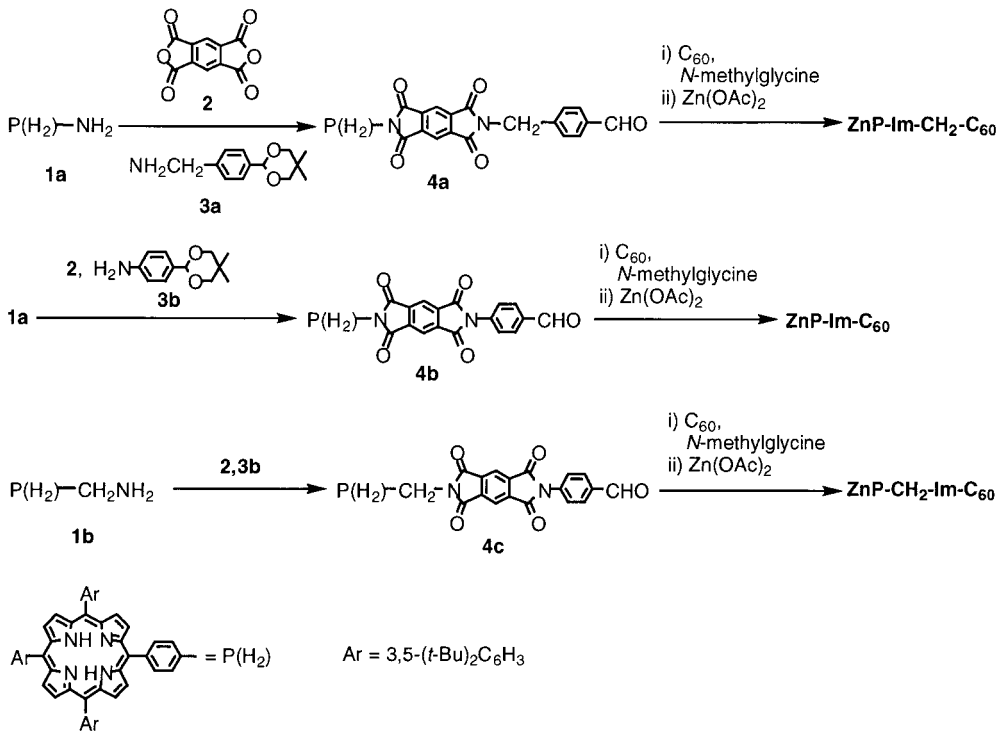

TABLE 1: One-Electron Redox Potentials (vs Fc/Fc^+)[a] of Triads in CH_2Cl_2 and Edge-to-Edge Distance (R_{ee}) and Center-to-Center Distance (R_{cc}) between Each Chromophore[b]

	redox potential			edge-to-edge distance (center-to-center distance)[b]		
	E^0_{ox}/V	E^0_{red}/V		R_{ee} (R_{cc}/Å)/Å		
compound	$ZnP^{\bullet+}/ZnP$	$C_{60}/C_{60}^{\bullet-}$	$Im/Im^{\bullet-}$	ZnP, Im	Im, C_{60}	ZnP, C_{60}
ZnP-Im-CH_2-C_{60}	+0.31	−1.13	−1.26	5.7 (12.5)	7.6 (13.4)	18.6 (25.3)
ZnP-Im-C_{60}	+0.31	−1.13	−1.21	5.7 (12.5)	6.5 (12.3)	18.4 (24.2)
ZnP-CH_2-Im-C_{60}	+0.32	−1.14	−1.26	6.4 (11.7)	6.5 (12.3)	16.3 (19.8)

[a] Measured by differential pulse voltammetry in CH_2Cl_2 using 0.1 M *n*-Bu_4NPF_6 as a supporting electrolyte with a sweep rate of 10 mV s^{-1}. [b] Estimated using molecular mechanics calculations (MacroModel, version 6.0).

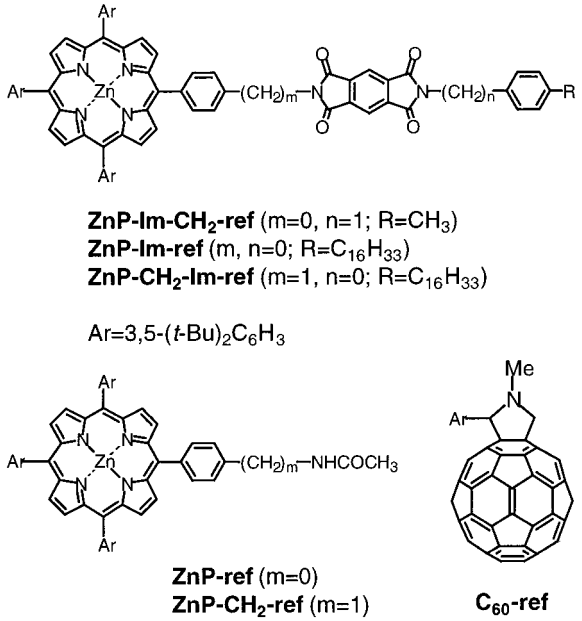

Figure 2. Porphyrin-pyromellitimide dyads and porphyrin and C_{60} references.

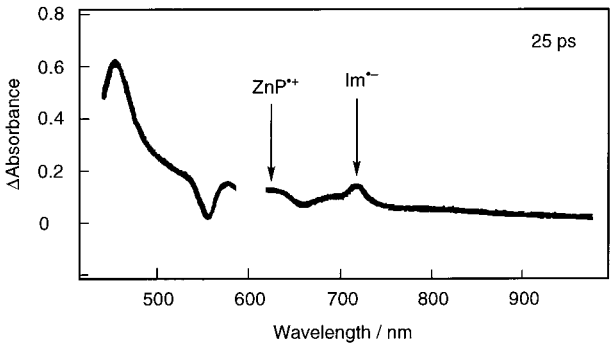

Figure 3. Differential absorption spectra obtained upon picosecond flash photolysis (590 nm) of $\sim 10^{-4}$ M solutions of **ZnP-Im-CH_2-ref** in argon saturated THF with a time delay of 25 ps.

ref in THF with a picosecond pulse at 590 nm (absorption ratio of porphyrin:C_{60}=14:1), transient absorption bands at 460, 620, and 710 nm appear, accompanied by bleaching of the ground-state porphyrin absorption at 560 nm, as shown in Figure 3. The transient absorption bands at 460 and 620 nm are characteristic of those of the zincporphyrin radical cation ($ZnP^{\bullet+}$),[32] and the band at 710 nm is diagnostic of the imide radical anion ($Im^{\bullet-}$).[33] The absorption that is due to the porphyrin excited singlet state ($^1ZnP^*$) is overlapped with the band at 460 nm. These results clearly reveal formation of the

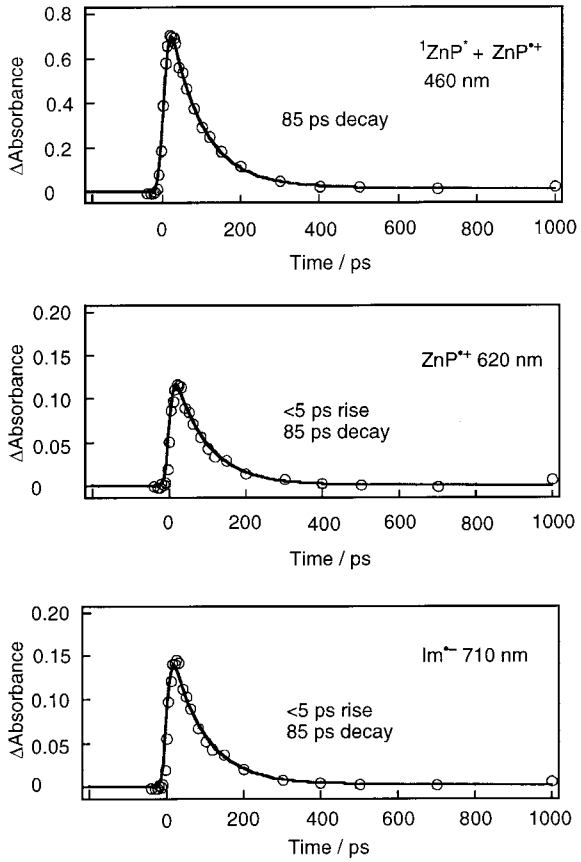

Figure 4. Time profiles in the transient absorption spectra of **ZnP-Im-CH_2-ref** in THF at 460 (top), 620 (middle), and 710 nm (bottom) in THF. The solid lines are the simulated curves by convolution of exciting pulse, transient absorption, and probing pulse with the lifetime of 85 and <5 ps (S1 and S2).

charge-separated state, i.e., the $ZnP^{\bullet+}$-$Im^{\bullet-}$ radical ion pair via photoinduced ET from the $^1ZnP^*$ to the Im moiety.

The time profile of the absorbance at 460 nm, which corresponds to the $^1ZnP^*$ and $ZnP^{\bullet+}$, was analyzed by a single-exponential decay with a lifetime of 85 ± 9 ps (Figure 4). The time profiles of the absorbance at 620 and 710 nm, which are due to $ZnP^{\bullet+}$ and $Im^{\bullet-}$, respectively, were fitted by a fast rise (<5 ps) and a decay (85 ± 9 ps) component (Figure 4). The fitting procedure of the kinetic data are given in the Supporting Information (S1 and S2). The fluorescence lifetimes of the porphyrin-pyromellitimide dyads were also measured by a picosecond single-photon counting technique (see the Experimental Section). The samples in THF were excited at 524 nm, where the porphyrin moiety absorbs mainly. The fluorescence decay was monitored at 605 nm, where the emission is due to

TABLE 2: CS ($k_{ET(CS)}$), CSH ($k_{ET(CSH)}$), and CR ($k_{ET(CR)}$) Rate Constants of Triads and Dyads Obtained Using Transient Absorption Spectroscopy, Quantum Yield (ϕ_1, ϕ_2, ϕ_{total}), and Activation Energy (E_a)

	$k_{ET(CS)}/s^{-1}$ [a] (ϕ_1) [b]		$k_{ET(CSH)}/s^{-1}$ [a] (ϕ_2) [b]		$k_{ET(CR)}/s^{-1}$ [a] ($\phi_{total} = \phi_1 \times \phi_2$) [b]		E_a/eV [d]
compound	THF	dioxane	THF	dioxane	THF	dioxane	THF
ZnP-Im-CH$_2$-C$_{60}$	1.3×10^{10} (0.97)	4.5×10^{9} (0.90)	7.0×10^{10} (<0.26)	2.8×10^{9} (0.11)	2.9×10^{6} (<0.25)	[c] (0.10)	0.13 [d]
ZnP-Im-CH$_2$-ref	1.1×10^{10} (0.96)	4.5×10^{9} (0.90)			$>2 \times 10^{11}$	2.2×10^{10}	
ZnP-Im-C$_{60}$	1.8×10^{10} (0.97)	7.8×10^{9} (0.94)	1.0×10^{11} (0.50)	1.6×10^{10} (0.48)	8.3×10^{5} (0.49)	[c] (0.45)	~0 [d]
ZnP-Im-ref	1.1×10^{10} (0.92)	5.1×10^{9} (0.91)			1.0×10^{11}	1.7×10^{10}	
ZnP-CH$_2$-Im-C$_{60}$	2.9×10^{9} (0.88)	1.7×10^{9} (0.59)	1.7×10^{10} (0.25)	4.4×10^{8} (0.37)	8.3×10^{5} (0.22)	[c] (0.22)	0.07 [d]
ZnP-CH$_2$-Im-ref	1.9×10^{9} (0.79)	8.0×10^{8} (0.32)			5.0×10^{10}	7.4×10^{8}	
ZnP-C$_{60}$ [e]					3.7×10^{5} [e] (0.99)		
ZnP-H$_2$P-C$_{60}$ [e]					2.9×10^{4} [e] (0.26)		

[a] The k_{ET} values were determined by analyzing the decay and rise of transient species (i.e., ^{1}ZnP*, ZnP$^{\bullet+}$, Im$^{\bullet-}$, and C$_{60}^{\bullet-}$) at 460, 620, 710, and 1000 nm. [b] The quantum yields of formation of charge-separated states were determined according to Schemes 2 and 3 [$\phi_1 = k_{ET(CS1)}/(k_{ET(CS1)} + k_0 + k_{ISC})$, $\phi_2 = k_{ET(CSH)}/(k_{ET(CSH)} + k_{ET(CR1)})$]. [c] The decay of the charge-separated state to the triplet excited states is much faster than that to the ground state. [d] The E_a values were determined from Arrhenius analyses of the temperature-dependent CR rates. [e] From ref 24c,e.

SCHEME 2: Reaction Scheme and Energy Diagram for ZnP-Im-CH$_2$-ref in THF

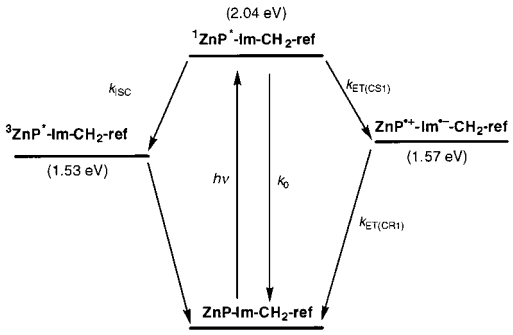

only the porphyrin moiety. The decay curves were fitted by a single exponential. On the basis of the fluorescence lifetimes of the dyads (τ) and the reference (**ZnP-ref**: τ_0), the CS rate constant ($k_{ET(CS1)}$) from the ^{1}ZnP* to the Im moiety was determined using eq 1. The fluorescence lifetime (τ)

$$k_{ET(CS1)} = \tau^{-1} - \tau_0^{-1} \quad (1)$$

of the ^{1}ZnP* moiety in **ZnP-Im-CH$_2$-ref** (77 ± 8 ps) agrees within experimental error with the lifetime of the radical ion pair (85 ± 9 ps) in Figure 4. Such an agreement indicates that the formation of the radical ion pair (**ZnP$^{\bullet+}$-Im$^{\bullet-}$-CH$_2$-ref**) via photoinduced ET from the ^{1}ZnP* to the Im moiety is the rate-determining step, followed by the fast CR to the ground state (<5 ps). In such a case, the concentration of **ZnP$^{\bullet+}$-Im$^{\bullet-}$-CH$_2$-ref** rapidly reaches a maximum within 5 ps and decays as ^{1}ZnP* disappears via the photoinduced ET with the same time constant as observed in Figure 4. Similar kinetic behavior has been reported in dyads consisting of porphyrin linked quinones[34] and imides.[35] Overall, photoinduced ET takes place from the porphyrin excited singlet state to the Im moiety, and in turn, the resulting ZnP$^{\bullet+}$-Im$^{\bullet-}$ ion pair recombines to regenerate the ground state as shown in Scheme 2.

The energetics shown in Scheme 2 are obtained from the one-electron redox potentials and the excitation energies of the electron donor and acceptor moieties (see the Experimental Section and the Supporting Information, S3).[36] The driving forces ($-\Delta G^0_{ET(CR)}$ in eV) for the intramolecular CR processes from the imide radical anion (Im$^{\bullet-}$) to the zincporphyrin radical cation (ZnP$^{\bullet+}$) in the dyads are determined by eq 2, where e stands for the elementary charge:

$$-\Delta G^0_{ET(CR)} = e[E^0_{ox}(D^{\bullet+}/D) - E^0_{red}(A/A^{\bullet-})] \quad (2)$$

The driving forces for the intramolecular CS processes ($-\Delta G^0_{ET(CS)}$ in eV) from the zinc porphyrin singlet excited state to the Im was determined by eq 3:

$$-\Delta G^0_{ET(CS)} = \Delta E_{0-0} + \Delta G^0_{ET(CR)} \quad (3)$$

where ΔE_{0-0} is the energy of the 0−0 transition energy gap between the lowest excited state and the ground state, which is determined by the 0−0* absorption and 0*−0 fluorescence maxima. It should be noted that the Coulombic terms in the present donor−acceptor systems are assumed to be negligible in solvents with moderate polarity (i.e., THF), because of the relatively long edge-to-edge distance employed.[36]

The photodynamical behavior of **ZnP-Im-ref** and **ZnP-CH$_2$-Im-ref** in THF was similar to those described in **ZnP-Im-CH$_2$-ref**. The rate constants of the CS ($k_{ET(CS1)}$) and the CR ($k_{ET(CR1)}$) were determined by analyzing the decay and rise of the absorbance as in the case of **ZnP-Im-CH$_2$-ref** (Figure 4). The quantum yields of formation of CS states (ϕ_1) were determined from the fluorescence lifetimes according to Scheme 2. The values of $k_{ET(CS1)}$, $k_{ET(CR1)}$, and ϕ_1 thus determined are summarized in Table 2.

The $k_{ET(CS1)}$ (1.1×10^{10} s^{-1}) and $k_{ET(CR1)}$ (1.0×10^{11} s^{-1}) values of **ZnP-Im-ref** without a methylene linkage are significantly larger than the $k_{ET(CS1)}$ (1.9×10^{9} s^{-1}) and $k_{ET(CR1)}$ (5.0×10^{10} s^{-1}) values of **ZnP-CH$_2$-Im-ref** with a methylene linkage, respectively. The incorporation of one methylene unit between the porphyrin and imide moieties renders the electronic coupling between the two chromophores smaller, thereby attenuating the ET rates of the latter as compared to those of the former. The photodynamical behavior of **ZnP-Im-CH$_2$-ref**, **ZnP-Im-ref**, and **ZnP-CH$_2$-Im-ref** in 1,4-dioxane was similar to those in THF, and the data are also given in Table 2.[37] It

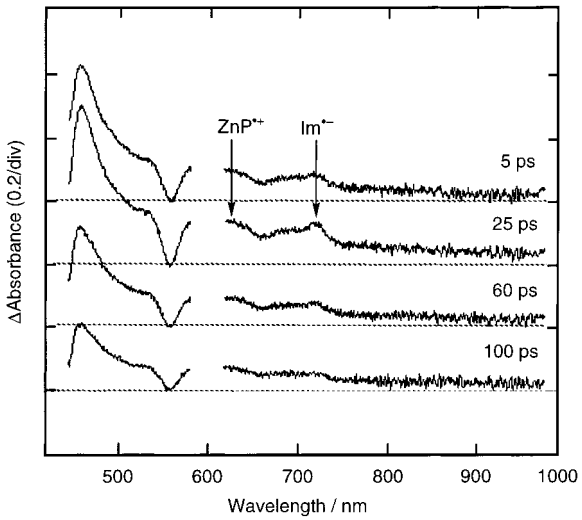

Figure 5. Differential absorption spectra obtained upon picosecond flash photolysis (590 nm) of ~10^{-4} M solutions of **ZnP-Im-CH$_2$-C$_{60}$** in argon saturated THF with a time delay of 5, 25, 60, and 100 ps.

SCHEME 3: Reaction Scheme and Energy Diagram for ZnP-Im-CH$_2$-C$_{60}$ in THF

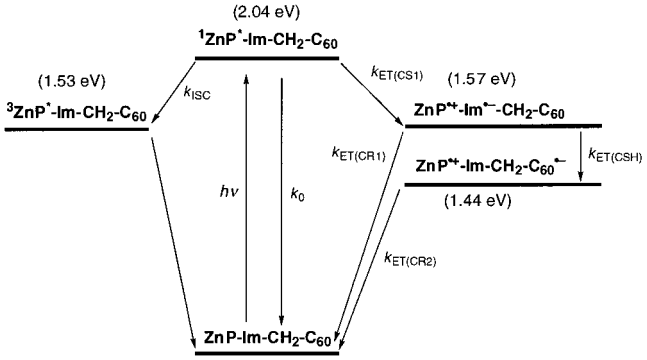

should be noted here that the relative ratios of $k_{ET(CR1)}$ vs $k_{ET(CS1)}$ in THF are much larger than those in 1,4-dioxane. The driving force ($-\Delta G_{ET(CR)}$) for the CR process decreases, and the reorganization energy increases with increasing the solvent polarity, rendering the CR rate larger in polar solvents. In contrast, both of the ET parameters for the CS process increase with increasing the solvent polarity, leaving the CS rate rather unchanged.[34] Therefore, the photodynamics of the triads were not examined in more polar solvents such as benzonitrile.

Photophysics of Porphyrin-Pyromellitimide-Fullerene Triads. The energy levels of the triads in THF are obtained from the one-electron redox potentials and the excitation energies of the electron donor and acceptor moieties (see the Experimental Section) as shown in Scheme 3 (**ZnP-Im-CH$_2$-C$_{60}$** as a representative example).

Figure 5 depicts the picosecond absorption spectra of **ZnP-Im-CH$_2$-C$_{60}$** in a THF solution (absorption ratio of ZnP:C$_{60}$=14:1). First, a fast step occurs, which involves CS from the ^{1}ZnP* to the Im moiety ($k_{ET(CS1)} = 1.3 \times 10^{10}$ s^{-1}, $\phi_1 = 0.97$), and second, a CSH reaction between the Im•− and the C$_{60}$ moieties occurs ($k_{ET(CSH)} = 7.0 \times 10^{10}$ s^{-1}, $\phi_2 < 0.26$).[38] The total quantum yield of the formation of the charge-separated state ($\phi_{total} = \phi_1 \times \phi_2$) is determined as <0.25 in THF. Similar photodynamical behavior was noted for **ZnP-Im-C$_{60}$** and **ZnP-CH$_2$-Im-C$_{60}$**, and the results are summarized in Table 2.[39]

The CS1 rate constant of **ZnP-CH$_2$-Im-C$_{60}$** (2.9×10^9 s^{-1}) in THF is smaller by 1 order of magnitude than those of **ZnP-Im-C$_{60}$** (1.8×10^{10} s^{-1}) and **ZnP-Im-CH$_2$-C$_{60}$** (1.3×10^{10} s^{-1}) in THF. This is virtually the same as that described in the dyads (vide supra). Similar deceleration in the CS1 rates of **ZnP-CH$_2$-Im-C$_{60}$** (1.7×10^9 s^{-1}) was observed in 1,4-dioxane as compared to those of **ZnP-Im-C$_{60}$** (7.8×10^9 s^{-1}) and **ZnP-Im-CH$_2$-C$_{60}$** (4.5×10^9 s^{-1}) in 1,4-dioxane (see the Supporting Information, S4−S6). Thus, the attenuation of the CS1 rate results from the weaker electronic coupling between the porphyrin and the imide moieties because of the existence of the additional methylene group within the spacer.

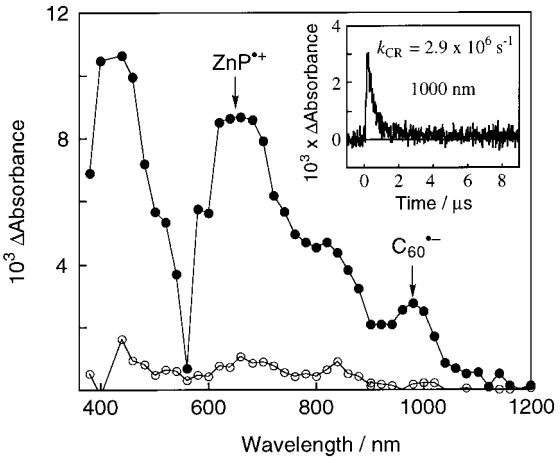

Figure 6. Differential absorption spectra obtained upon nanosecond flash photolysis (550 nm) of ~10^{-4} M solutions of **ZnP-Im-CH$_2$-C$_{60}$** in argon saturated THF with a time delay of 200 ns (black circles) and 2 μs (open circles). The time profile of absorbance at 1000 nm at 273 K is shown as the inset.

The CSH rate constant of **ZnP-Im-CH$_2$-C$_{60}$** in THF (7.0×10^{10} s^{-1}) is smaller than that of **ZnP-Im-C$_{60}$** in THF (1.0×10^{11} s^{-1}) despite of the slightly large driving force ($-\Delta G_{ET(CSH)} = 0.13$ eV) for the former relative to the latter ($-\Delta G_{ET(CSH)} = 0.08$ eV). This can be accommodated by the small electronic coupling of the former as compared to the latter because of the incorporation of an additional methylene group between the Im and the C$_{60}$ moieties.[40] It should be noted here that, despite the small driving force for the CSH (0.08−0.13 eV), the CSH process competes well with the CR1 process, resulting in the formation of the final charge-separated state (i.e., **ZnP•+-(CH$_2$)$_m$-Im-(CH$_2$)$_n$-C$_{60}$•−**). Osuka et al. reported sequential ET in similar zincporphyrin-pyromellitimide-quinone (ZnP-Im-Q) triads where a short methylene spacer is employed between the imide and the quinone moieties.[33] Provided that there is a similar driving force for the CSH reaction (0.07−0.24 eV) with the short methylene spacer, the CSH rate from the imide to the quinone in THF is estimated as 10^9−10^{10} s^{-1}, which is comparable to the CSH value (1.7×10^{10} s^{-1}) of the corresponding triad (**ZnP-CH$_2$-Im-C$_{60}$**) in THF. Taking into account the stronger electronic coupling of the CSH process in ZnP-Im-Q versus **ZnP-CH$_2$-Im-C$_{60}$**, the fast CSH in the present systems can be attributed to the small reorganization energy of the C$_{60}$ relative to the imide.[27c]

Formation of C$_{60}$•− (1000 nm) and ZnP•+ (broad absorption around 620 nm) in **ZnP-Im-CH$_2$-C$_{60}$** was substantiated by a set of complementary nanosecond laser photolysis experiments (550 nm), as shown in Figure 6. The decay of both the absorption bands (1000 and 620 nm) obeys clean first-order kinetics with decay rate constants that are virtually identical for both radical species. No characteristic absorption because of the Im•− was detected as an intermediate species. This demonstrates that an intramolecular CR from C$_{60}$•− to ZnP•+ governs the fate of **ZnP•+-Im-CH$_2$-C$_{60}$•−**. The CR rate constants

CHART 1

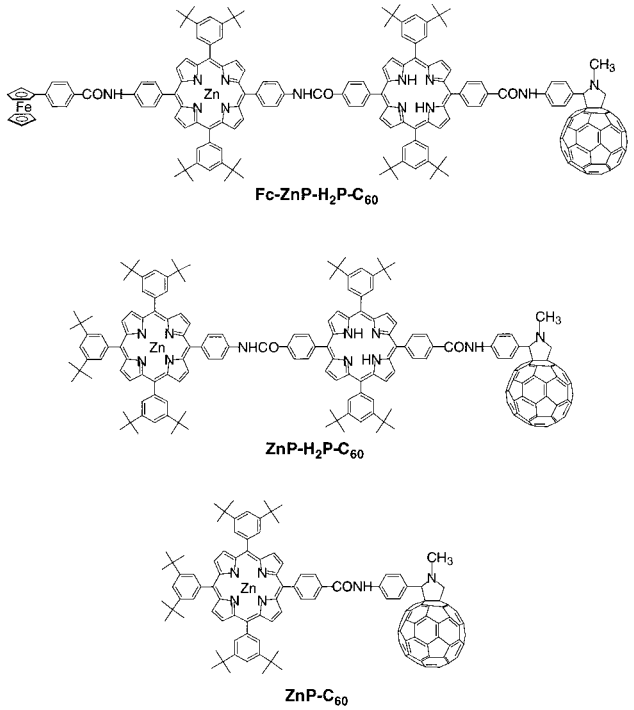

($k_{ET(CR2)}$) of **ZnP-Im-CH$_2$-C$_{60}$**, **ZnP-Im-C$_{60}$**, and **ZnP-CH$_2$-Im-C$_{60}$** in THF at 273 K thus determined are listed in Table 2. In contrast to the CR process in THF, no formation of $C_{60}^{\bullet-}$ (1000 nm) and $ZnP^{\bullet+}$ (broad absorption around 620 nm) in the longer time scale than 10 ns was detected for **ZnP-Im-CH$_2$-C$_{60}$** in 1,4-dioxane (the dielectric constant: $\epsilon_s = 2.2$) which is less polar than THF ($\epsilon_s = 7.58$).[41] In 1,4-dioxane, the energy level of the radical ion pair, **ZnP$^{\bullet+}$-Im-CH$_2$-C$_{60}^{\bullet-}$**, is higher than the triplet excited states of C_{60} ($^3C_{60}^*$) and ZnP ($^3ZnP^*$), and thus, the decay of the CS state results in formation of $^3C_{60}^*$ and $^3ZnP^*$, which are detected as the triplet−triplet absorption spectra of $^3C_{60}^*$ (700 nm)[23,42] and $^3ZnP^*$ (740 and 840 nm)[23,42] upon nanosecond laser flash photolysis of **ZnP-Im-CH$_2$-C$_{60}$** in 1,4-dioxane (See the Supporting Information, S6).[43]

The $k_{ET(CR2)}$ values of **ZnP-Im-C$_{60}$** (8.3×10^5 s^{-1}) and **ZnP-CH$_2$-Im-C$_{60}$** (8.3×10^5 s^{-1}) in THF are identical, but they are smaller by a factor of 3 than that of **ZnP-Im-CH$_2$-C$_{60}$** (2.9×10^6 s^{-1}). We have reported the relationship between the edge-to-edge distance (R_{ee}) and the optimal ET rate constant ($k_{ET(optimal)}$) in a homologous series of porphyrin-linked fullerene systems [i.e., zincporphyrin-fullerene dyad (**ZnP-C$_{60}$** (R_{ee}=11.9 Å)), zincporphyrin-freebase porphyrin-fullerene triad (**ZnP-H$_2$P−C$_{60}$** (R_{ee}=30.3 Å)), and ferrocene-zincporphyrin-freebase porphyrin-fullerene triad (**Fc-ZnP-H$_2$P-C$_{60}$** (R_{ee}=48.6 Å)); Chart 1].[24c,e] The $k_{ET(optimal)}$ values are correlated with the R_{ee} values to yield the decay coefficient factor [damping factor (β) = 0.60 Å^{-1}], which is located within the boundaries of nonadiabatic ET reactions for saturated hydrocarbon bridges (0.8−1.0 Å^{-1}) and unsaturated phenylene bridges (0.4 Å^{-1}).[44] Taking into account the above experimental results, we can estimate the k_{CR2} values in the present systems (R_{ee} = 16.3−18.6 Å) as $(0.6-2) \times 10^5$ s^{-1}, which is smaller by 1 order of magnitude than the experimental values [$(0.83-2.9) \times 10^6$ s^{-1}]. This indicates that the CR mechanism in porphyrin-pyromellitimide-fullelere triads is different from that reported for porphyrin-linked fullerene systems[24c,e,45] (vide infra).

Sequential vs Superexchange Charge Recombination. Temperature dependence of the intramolecular CR rates from the $C_{60}^{\bullet-}$ to the $ZnP^{\bullet+}$ in the triads was examined in THF. Arrhenius plots of the k_{CR2} values display a drastic trend in the triads, as shown in Figure 7. There is a good linear correlation between ln(k_{CR2}) and T^{-1} for **ZnP$^{\bullet+}$-Im-CH$_2$-C$_{60}^{\bullet-}$** (Figure 7a). The activation energy (E_a) derived from the slope (0.13 eV) agrees with the difference in the energy level between **ZnP$^{\bullet+}$-Im$^{\bullet-}$-CH$_2$-C$_{60}$** and **ZnP$^{\bullet+}$-Im-CH$_2$-C$_{60}^{\bullet-}$** (0.13 eV in Scheme 3). Such an agreement strongly indicates that the CR2 process proceeds via a *sequential* ET pathway through the intermediate, **ZnP$^{\bullet+}$-Im$^{\bullet-}$-CH$_2$-C$_{60}$**, which is by 0.13 eV higher in energy than **ZnP$^{\bullet+}$-Im-CH$_2$-C$_{60}^{\bullet-}$** followed by ET from $Im^{\bullet-}$ to $ZnP^{\bullet+}$. Such a sequential ET may be preferred because of the weak electronic coupling at the relatively long distance (R_{ee} = 18.6 Å; vide infra).

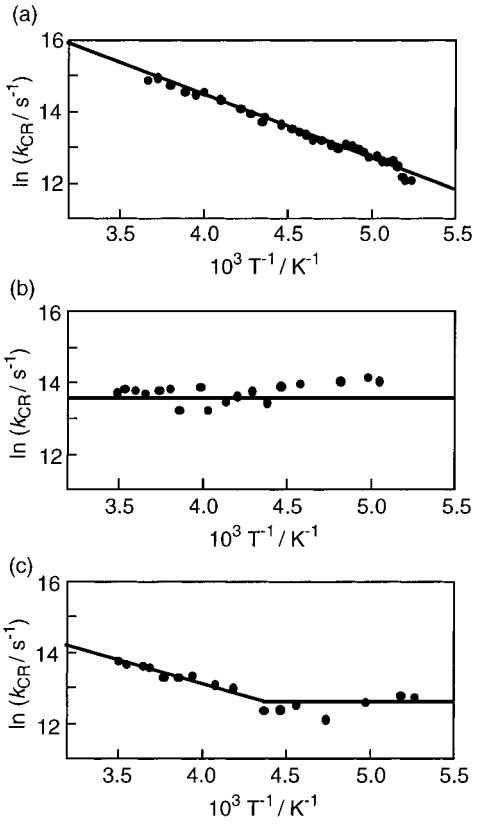

Figure 7. Arrhenius plots of k_{CR} for the intramolecular CR process from $C_{60}^{\bullet-}$ to $ZnP^{\bullet+}$ in (a) **ZnP-Im-CH$_2$-C$_{60}$**, (b) **ZnP-Im-C$_{60}$**, and (c) **ZnP-CH$_2$-Im-C$_{60}$** in THF.

In contrast to such a thermally activated CR, the k_{CR2} value of **ZnP-Im-C$_{60}$** remains a nearly temperature-independent value (Figure 7b). Such a temperature independence of k_{CR2} strongly suggests that the CR2 process in **ZnP-Im-C$_{60}$** does not proceeds over a thermally activated barrier but proceeds directly through electron tunneling via superexchange.[45] The relatively strong electron coupling without methylene linkage in **ZnP-Im-C$_{60}$** may result in such preference of the superexchange ET over the sequential ET which requires the thermal activation to reach the higher energy state of **ZnP$^{\bullet+}$-Im$^{\bullet-}$-C$_{60}$** (vide infra). On the other hand, the temperature dependence of k_{CR2} of **ZnP-CH$_2$-Im-C$_{60}$** shows both behaviors: there is an Arrhenius-like temperature dependence at higher temperatures, but below 230 K, the k_{CR2} value becomes a temperature-independent value (Figure 7c). The temperature-independent k_{CR2} value of **ZnP-CH$_2$-Im-C$_{60}$** is smaller than the value of **ZnP-Im-C$_{60}$** because of the weaker electron coupling with the methylene linkage.[46]

Assuming that the Franck−Condon factor is similar throughout the series and the CR takes place mainly through the σ and

π bonds of the linkage, the observed temperature dependence of k_{CR2} can be rationalized by the following superexchange mechanism.[47,48] The superexchange coupling, V_{se}, between a donor (D) state (d) and an acceptor (A) state (a) via a bridge (B) state (b) is given by eq 4:

$$V_{se} = (V_{db}\, V_{ba})/\Delta E_{db} \quad (4)$$

where V_{db} and V_{ba} are respective electronic coupling between d and b and b and a and ΔE_{db} is the energy difference between the states d and b. The bridged state b is a virtual state which simply increases the electronic coupling between the D and A states by mixing with them. In superexchange-mediated CR of the present systems, the process could involve the following transfers: an ET from the SOMO of the $C_{60}^{\bullet-}$ (D) to the SOMO of the $ZnP^{\bullet+}$ (A), mediated by the LUMO of the Im (B).

On the basis of the $-\Delta G_{ET(CSH)}$ values in THF, ΔE_{db} values are in the order of **ZnP-Im-CH_2-C_{60}** ≈ **ZnP-CH_2-Im-C_{60}** > **ZnP-Im-C_{60}**. Taking into account the effect of a methylene group on the electronic coupling, V_{db} and V_{ba} are in the order of **ZnP-CH_2-Im-C_{60}** ≈ **ZnP-Im-C_{60}** > **ZnP-Im-CH_2-C_{60}** and **ZnP-Im-CH_2-C_{60}** ≈ **ZnP-Im-C_{60}** > **ZnP-CH_2-Im-C_{60}**, respectively. Thus, the V_{se} value of **ZnP-Im-C_{60}** is much larger than those of **ZnP-CH_2-Im-C_{60}** and **ZnP-Im-CH_2-C_{60}**. This is consistent with the experimental results in that no temperature dependence of the CR2 rate in **ZnP-Im-C_{60}** was observed.

In conclusion, this study has demonstrated for the first time that a subtle change of the linkage between the donor and acceptor moieties causes a drastic switch between the sequential and superexchange-mediated CR as well as the modulation of the CS process.

Experimental Section

General. Melting points were recorded on a Yanagimoto micro-melting-point apparatus and not corrected. ^{1}H NMR spectra were measured on a JEOL EX-270. Fast atom bombardment mass spectra (FABMS) were obtained on a JEOL JMS-DX300. Matrix-assisted laser desorption/ionization (MALDI) time-of-flight mass spectra (TOF) were measured on a Kratos Compact MALDI I (Shimadzu). IR spectra were measured on a Perkin-Elmer FT-IR 2000 spectrophotometer as KBr disks. Steady-state absorption spectra in the visible and near-IR regions were measured on a Jasco V570 DS spectrophotometer. Elemental analyses were performed on a Perkin-Elmer model 240C elemental analyzer. The edge-to-edge (R_{ee}) and center-to-center (R_{cc}) distances were determined from molecular modeling using MM3 (MacroModel, version 6.0).

Materials. All solvents and chemicals were of reagent grade quality, obtained commercially and used without further purification except as noted below. Tetrabutylammonium hexafluorophosphate used as a supporting electrolyte for the electrochemical measurements was obtained from Tokyo Kasei Organic Chemicals. THF and DMF were purchased from Wako Pure Chemical Ind., Ltd., and purified by successive distillation over calcium hydride. Dichloromethane was refluxed and distilled from P_2O_5. Thin-layer chromatography (TLC) and flash column chromatography were performed with Art. 5554 DC-Alufolien Kieselgel 60 F_{254} (Merck) and Fujisilicia BW300, respectively.

Synthesis of Porphyrin-Fullerene Linked Molecules and the References. 4b. 5-(4-Aminophenyl)-10,15,20-tris(3,5-di-*tert*-butylphenyl)porphyrin **1a** (96.5 mg, 0.100 mmol), pyromellitic dianhydride **2** (22.0 mg, 0.100 mmol), and 2-(4-aminophenyl)-5,5-dimethyl-1,3-dioxane **3b** (21.0 mg, 0.100 mmol) in dry DMF (15 mL) were heated at reflux under an atmospheric pressure of nitrogen in the dark for 16 h. The reaction mixture was allowed to cool to room temperature and then evaporated to dryness at a reduced pressure. TLC showed several porphyrin bands (benzene), and the fourth band (R_f = 0.9, chloroform/methanol (9:1)) was separated by flash column chromatography. The fraction was concentrated and dissolved in a mixture of chloroform (10 mL), trifluoroacetic acid (4 mL), and 5% aqueous sulfuric acid (3 mL). After it was stirred for 12 h, the mixture was poured into 30 mL of water and extracted with $CHCl_3$. The organic layer was washed with saturated $NaHCO_3$ aqueous solution, dried over anhydrous Na_2SO_4, and evaporated. Flash column chromatography on silica gel with chloroform as an eluent (R_f = 0.45, chloroform) and subsequent reprecipitation from benzene/methanol gave **4b** as a black red solid (24.1 mg, 0.0190 mmol, 19%). mp > 300 °C; ^{1}H NMR (270 MHz, $CDCl_3$) δ 10.11 (s, 1H), 8.94 (d, J = 5 Hz, 2H), 8.93 (s, 4H), 8.91 (d, J = 5 Hz, 2H), 8.43 (d, J = 8 Hz, 2H), 8.31 (s, 2H), 8.13 (d, J = 2 Hz, 4H), 8.11 (d, J = 2 Hz, 2H), 8.08 (d, J = 8 Hz, 2H), 7.88 (d, J = 8 Hz, 2H), 7.82 (t, J = 2 Hz, 2H), 7.81 (t, J = 2 Hz, 1H), 7.75 (d, J = 8 Hz, 2H), 1.54 (s, 54H), −2.76 (br.s, 2H); MS(FAB) 1271 ($M + H^+$); FTIR (KBr) 3737, 1734, 1654, 1559, 1542, 1508, 1474, 1362, 802, 669 cm^{-1}.

ZnP-Im-C_{60}. C_{60} (37.4 mg, 0.0520 mmol), **4b** (22.0 mg, 0.0173 mmol), and *N*-methylglycine (46.3 mg, 0.520 mmol) in dry toluene (11 mL) were heated at reflux under an atmospheric pressure of nitrogen in the dark for 6 h. The reaction mixture was allowed to cool to room temperature and then evaporated to dryness at a reduced pressure. Flash column chromatography on silica gel with chloroform as an eluent (R_f = 0.35, chloroform) and subsequent reprecipitation from benzene/methanol gave the desired product as a black red solid (11.5 mg, 5.71 μmol, 33%). mp > 300 °C; ^{1}H NMR (270 MHz, $CDCl_3$) δ 8.95 (d, J = 5 Hz, 2H), 8.92 (d, J = 5 Hz, 4H), 8.89 (d, J = 5 Hz, 2H), 8.44 (s, 2H), 8.36 (d, J = 8 Hz, 2H), 8.12 (d, J = 2 Hz, 4H), 8.06 (d, J = 2 Hz, 2H), 7.92 (d, J = 8 Hz, 2H), 7.83 (br.s, 2H), 7.81 (t, J = 2 Hz, 2H), 7.78 (t, J = 2 Hz, 1H), 7.64 (d, J = 8 Hz, 2H), 4.63 (d, J = 10 Hz, 1H), 4.52 (s, 1H), 3.85 (d, J = 10 Hz, 1H), 2.72 (s, 3H), 1.55 (s, 54H), −2.71 (br.s, 2H); MS (FAB) MS (FAB) 721 (C_{60}), 1298 $[M - C_{60}]^+$; FTIR (KBr) 3747, 1731, 1591, 1514, 1455, 1361, 1089, 1001, 797, 718, 527 cm^{-1}; ^{13}C NMR (68 MHz, $CDCl_3$, The symbol * means several superimposed signals.) δ 164.92, 164.70, 148.70, 148.53, 145.5−143.9*, 140.3−141.7*, 138.49*, 137.02*, 135.06, 133.77, 130.8−131.8*, 130.87, 130.39, 129.95, 129.55, 125.99, 124.45, 121.83, 121.56, 121.00, 118.88. 118.63, 117.90, 82.41 (−*C*H−Ph), 77.13 (C_{60}-sp^3), 69.41 (−*C*H_2−), 67.89 (C_{60}-sp^3), 40.08 (N−*C*H_3), 35.20 (−*C*$(CH_3)_3$), 35.13 (−*C*$(CH_3)_3$), 31.95 (−*C*$(CH_3)_3$), 31.89 (−*C*$(CH_3)_3$). Some of the ^{13}C NMR signals could not be assigned because of the overlapping with the solvent peaks. A saturated methanol solution of $Zn(OAc)_2$ (3 mL) was added to a solution of the sample of the C_{60} adduct (10.0 mg, 4.96 μmol) in $CHCl_3$ (30 mL) and heated at reflux for 30 min. After cooling, the reaction mixture was washed with water twice and dried over anhydrous Na_2SO_4, and then the solvent was evaporated. Flash column chromatography on silica gel with $CHCl_3$ as an eluent and subsequent reprecipitation from benzene-methanol gave **ZnP-Im-C_{60}** as a brown solid (100% yield, 10.3 mg, 4.96 μmol). mp > 300 °C; ^{1}H NMR (270 MHz, $CDCl_3$) δ 9.05 (d, J = 5 Hz, 4H), 9.03 (d, J = 5 Hz, 2H), 9.01 (d, J = 5 Hz, 2H), 8.97 (d, J = 5 Hz, 2H), 8.40 (s, 2H), 8.33 (d, J = 8 Hz, 2H), 8.11 (d, J = 2 Hz, 4H), 8.04 (d, J = 2 Hz, 2H), 7.92 (d, J = 8 Hz, 2H), 7.81 (t, J = 2 Hz, 2H), 7.76 (t, J

= 2 Hz, 1H), 7.72 (br.s, 2H), 7.62 (d, J = 8 Hz, 2H), 4.42 (d, J = 10 Hz, 1H), 4.25 (s, 1H), 3.63 (d, J = 10 Hz, 1H), 2.66 (s, 3H), 1.56 (s, 54H); MS (FAB) 721 (C_{60}), 1360 $[M - C_{60}]^+$; IR (KBr) 1731, 1591, 1514, 1455, 1361, 1089, 1001, 797, 718, 527 cm^{-1}; ^{13}C NMR (68 MHz, $CDCl_3$) δ 165.38, 165.10, 150.56, 150.44, 150.36, 149.68, 148.64, 148.52, 146.75, 145.70, 145.52, 145.31, 144.78, 144.53, 143.71, 141.83, 141.09, 137.30, 137.27, 135.07, 135.07, 132.64, 132.44, 132.44, 132.28, 131.52, 129.89, 129.54, 128.34, 126.13, 124.41, 122.66, 120.87, 120.82, 119.17, 82.63 ($-CH-$Ph), 77.76 (C_{60}-sp^3), 69.65 ($-CH_2-$), 68.39 (C_{60}-sp^3), 40.05 (N$-CH_3$), 35.06 ($-C(CH_3)_3$), 32.03 ($-C(CH_3)_3$).

ZnP-Im-ref. Aminoporphyrin **1a** (193 mg, 0.200 mmol), pyromellitic dianhydride **2** (44.0 mg, 0.200 mmol), and 4-hexadecylaniline (63.0 mg, 0.200 mmol) in dry DMF (30 mL) were heated at reflux under an atmospheric pressure of nitrogen in the dark for 22 h. The reaction mixture was allowed to cool to room temperature and then evaporated to dryness at a reduced pressure. TLC showed two porphyrin bands (R_f = 0.55 and 0.45, benzene), and the second band was separated by flash column chromatography. Reprecipitation from benzene/methanol gave the desired product as a black red solid (76.5 mg, 0.0523 mmol, 26%). mp > 300 °C; ^1H NMR (270 MHz, $CDCl_3$) δ 8.93 (d, J = 5 Hz, 2H), 8.92 (s, 4H), 8.90 (d, J = 5 Hz, 2H), 8.49 (s, 2H), 8.42 (d, J = 8 Hz, 2H), 8.11 (d, J = 2 Hz, 4H), 8.09 (d, J = 2 Hz, 2H), 7.90 (d, J = 8 Hz, 2H), 7.81 (t, J = 2 Hz, 2H), 7.80 (t, J = 2 Hz, 1H), 7.39 (d, J = 8 Hz, 2H), 7.37 (d, J = 8 Hz, 2H), 2.69 (t, J = 8 Hz, 2H),1.68 (m, 2H), 1.56 (s, 54H), 1.27 (m, 26H), 0.89 (t, J = 8 Hz, 3H), −2.72 (br.s, 2H); MS (FAB) 1467 ($M + H^+$); FTIR (KBr) 3733, 1732, 1559, 1593, 1557, 1515, 1471, 1363, 1247, 1094, 973, 914, 880, 802, 722, 668 cm^{-1}. A saturated methanol solution of $Zn(OAc)_2$ (3 mL) was added to a solution of the sample of the dyad (10.0 mg, 6.83 μmol) in $CHCl_3$ (30 mL) and heated at reflux for 30 min. After cooling, the reaction mixture was washed with water twice and dried over anhydrous Na_2SO_4, and then the solvent was evaporated. Flash column chromatography on silica gel with $CHCl_3$ as an eluent and subsequent reprecipitation from chloroform/methanol gave **ZnP-Im-ref** as a black red solid (100% yield, 10.3 mg, 6.83 μmol). mp > 300 °C; ^1H NMR (270 MHz, $CDCl_3$) δ 9.04 (d, J = 5 Hz, 2H), 9.03 (s, 4H), 9.01 (d, J = 5 Hz, 2), 8.55 (s, 2H), 8.43 (d, J = 8 Hz, 2H), 8.12 (d, J = 2 Hz, 4H), 8.10 (d, J = 2 Hz, 2H), 7.90 (d, J = 8 Hz, 2H), 7.81 (t, J = 2 Hz, 2H), 7.79 (t, J = 2 Hz, 1H), 7.39 (d, J = 8 Hz, 2H), 7.38 (d, J = 8 Hz, 2H), 2.69 (t, J = 8 Hz, 2H), 1.66 (m, 2H), 1.56 (s, 54H), 1.34 (m, 26H), 0.89 (t, J = 8 Hz, 3H); MS (FAB) 1531 ($M + H^+$); IR (KBr) 1731, 1593, 1514, 1466, 1364, 1290, 1248, 1219, 1094, 1002, 930, 880, 824, 799, 723 cm^{-1}.

3a. To a stirred solution of $LiAlH_4$ (5.57 g, 149 mmol) in dry THF (100 mL) was added a solution of 2-(4-cyanophenyl)-5,5-dimethyl-1,3-dioxane[29] (5.56 g, 25.6 mmol) in dry THF (40 mL) dropwise at 0 °C, and stirring was continued at 0 °C for 2 h. The reaction mixture was quenched by addition of 5 mL of ethyl acetate followed by addition of 60 mL of 3 M HCl aqueous solution. The organic layer was separated, washed with saturated Na_2CO_3, and dried over anhydrous Na_2SO_4, and then the solvent was evaporated. Flash column chromatography on silica gel with ethyl acetate/ethanol (4:1) as an eluent and subsequent reprecipitation from hexane/benzene gave **3a** as a pale yellow solid (73% yield, 4.16 g, 4.16 mmol). mp 115.2−116.2 °C; ^1H NMR (270 MHz, $CDCl_3$) δ 7.48 (d, J = 8 Hz, 2H), 7.31 (d, J = 8 Hz, 2H), 5.39 (s, 1H), 3.86 (s, 2H), 3.77 (d, J = 11 Hz, 2H), 3.65 (d, J = 11 Hz, 2H), 1.57 (s, 2H), 1.30 (s, 3H), 0.80 (s, 3H); MS (FAB) 222 ($M + H^+$); IR (KBr) 1611, 1471, 1381, 1315, 1214, 1033, 825, 790, 764, 712 cm^{-1}. Found: C, 70.7; H, 8.54; N, 5.96%. Calcd for $C_{14}H_{17}NO_2$: C, 70.6; H, 8.65; N, 6.33%.

4a. This compound was synthesized from **1a**, **2**, and **3a** by the same method as that described for **4b**. **4a** as a black red solid from benzene/methanol (25% yield); mp > 300 °C; ^1H NMR (270 MHz, $CDCl_3$) δ 9.99 (s, 1H), 8.93 (d, J = 5 Hz, 2H), 8.92 (s, 4H), 8.90 (d, J = 5 Hz, 2H), 8.41 (d, J = 8 Hz, 2H), 8.16 (s, 2H), 8.13 (s, 4H), 8.11 (s, 2H), 7.87 (d, J = 8 Hz, 2H), 7.86 (d, J = 8 Hz, 2H), 7.81 (s, 3H), 7.57 (d, J = 8 Hz, 2H), 4.89 (s, 2H), 1.54 (s, 54H), −2.78 (br.s, 2H); MS(FAB) 1284 ($M + H^+$); FTIR (KBr) 1730, 1476, 1362, 1254, 1095, 974, 917, 914, 899, 882, 802, 717 cm^{-1}.

ZnP-Im-CH_2-C_{60}. C_{60} (56.3 mg, 0.0781 mmol), **4a** (33.0 mg, 0.0257 mmol), and *N*-methylglycine (69.4 mg, 0.779 mmol) in dry toluene (20 mL) were heated at reflux under an atmospheric pressure of nitrogen in the dark for 19 h. The reaction mixture was allowed to cool to room temperature and then evaporated to dryness at a reduced pressure. Flash column chromatography on silica gel with chloroform as an eluent (R_f = 0.15, chloroform) and subsequent reprecipitation from chloroform/methanol gave the desired product as a dark grayish violet solid (25.0 mg, 0.0153 mmol, 60%). mp > 300 °C; ^1H NMR (270 MHz, $CDCl_3$) δ 8.91 (s, 8H), 8.44 (d, J = 8 Hz, 2H), 8.39 (s, 2H), 8.09 (s, 6H), 7.88 (d, J = 8 Hz, 2H), 7.80 (s, 3H), 7.76 (br.s, 2H), 7.53 (d, J = 8 Hz, 2H), 4.94 (s, 1H), 4.90 (d, J = 10 Hz, 1H), 4.17 (d, J = 10 Hz, 1H), 2.77 (s, 3H), 1.54 (s, 54H), −2.72 (br.s, 2H); MS (MALDI−TOF) 2026 ($M + H^+$); FTIR (KBr) 3745, 1725, 1592, 1457, 1363, 1095, 1002, 998, 718, 527 cm^{-1}. A saturated methanol solution of $Zn(OAc)_2$ (3 mL) was added to a solution of the sample of the C_{60} adduct (10.3 mg, 5.07 μmol) in $CHCl_3$ (30 mL) and heated at reflux for 30 min. After cooling, the reaction mixture was washed with water twice and dried over anhydrous Na_2SO_4, and then the solvent was evaporated. Flash column chromatography on silica gel with $CHCl_3$ as an eluent (R_f = 0.15, chloroform) and subsequent reprecipitation from chloroform/methanol gave **ZnP-Im-CH_2-C_{60}** as a dark violet solid (38% yield, 4.0 mg, 1.9 μmol). mp > 300 °C; ^1H NMR (270 MHz, $CDCl_3$) δ 9.02 (d, J = 5 Hz, 2H), 9.00 (s, 4H), 8.99 (d, J = 5 Hz, 2H), 8.48 (s, 2H), 8.41 (d, J = 8 Hz, 2H), 8.08 (d, J = 2 Hz, 6H), 7.91 (d, J = 8 Hz, 2H), 7.80 (t, J = 2 Hz, 2H), 7.79 (t, J = 2 Hz, 1H), 7.72 (br.s, 2H), 7.54 (t, J = 8 Hz, 1H), 4.94 (s, 2H), 4.81 (d, J = 10 Hz, 1H), 4.79 (s, 1H), 4.08 (d, J = 10 Hz, 1H), 2.76 (s, 3H), 1.53 (s, 54H); MS (MALDI−TOF) 2095 ($M + H^+$); FTIR (KBr) 1725, 1591, 1457, 1362, 1091, 1002, 798, 718, 527 cm^{-1}.

ZnP−Im-CH_2-ref. Aminoporphyrin **1a** (71.9 mg, 0.0744 mmol), pyromellitic dianhydride **2** (17.3 mg, 0.0793 mmol), and 4-methylbenzylamine (10.2 mg, 0.0842 mmol) in dry DMF (11 mL) were heated at reflux under an atmospheric pressure of nitrogen in the dark for 25 h. The reaction mixture was allowed to cool to room temperature and then evaporated to dryness at a reduced pressure. TLC showed three porphyrin bands (R_f = 0.65, 0.15, and 0.05, chloroform), and the second band was separated by flash column chromatography. Reprecipitation from benzene/methanol gave the desired product as a dark violet solid (20.4 mg, 0.0161 mmol, 22%). mp > 300 °C; ^1H NMR (270 MHz, $CDCl_3$) δ 8.93 (d, J = 5 Hz, 2H), 8.92 (s, 4H), 8.91 (d, J = 5 Hz, 2H), 8.41 (d, J = 8 Hz, 2H), 8.32 (s, 2H), 8.10 (d, J = 2 Hz, 4H), 8.09 (d, J = 2 Hz, 2H), 7.86 (d, J = 8 Hz, 2H), 7.80 (t, J = 2 Hz, 2H), 7.79 (t, J = 2 Hz, 1H), 7.37 (d, J = 8 Hz, 2H), 7.17 (d, J = 8 Hz, 2H), 4.87 (s, 2H), 2.34 (s, 3H), 1.54 (s, 54H), −2.74 (br.s, 2H); MS (FAB)

1270 (M + H$^+$); FTIR (KBr) 3774, 1725, 1593, 1476, 1370, 1247, 1095, 973, 917, 882, 802, 721 cm^{-1}. A saturated methanol solution of $Zn(OAc)_2$ (3 mL) was added to a solution of the sample of the dyad (40.5 mg, 0.0319 mmol) in $CHCl_3$ (190 mL) and heated at reflux for 30 min. After cooling, the reaction mixture was washed with water twice and dried over anhydrous Na_2SO_4, and then the solvent was evaporated. Flash column chromatography on silica gel with $CHCl_3$ as an eluent (R_f = 0.25, chloroform) and subsequent reprecipitation from chloroform/methanol gave **ZnP-Im-CH$_2$-ref** as a black red solid (75% yield, 31.7 mg, 0.0238 mmol). mp > 300 °C; ^{1}H NMR (270 MHz, $CDCl_3$) δ 9.03 (d, J = 5 Hz, 2H), 9.02 (s, 4H), 9.00 (d, J = 5 Hz, 2H), 8.45 (s, 2H), 8.41 (d, J = 8 Hz, 2H), 8.10 (d, J = 2 Hz, 4H), 8.09 (d, J = 2 Hz, 2H), 7.87 (d, J = 8 Hz, 2H), 7.80 (t, J = 2 Hz, 2H), 7.79 (t, J = 2 Hz, 1H), 7.39 (d, J = 8 Hz, 2H), 7.39 (d, J = 8 Hz, 2H), 7.18 (d, J = 8 Hz, 2H), 4.90 (s, 2H), 2.34 (s, 3H), 1.53 (s, 54H); MS (FAB) 1332 (M + H$^+$); FTIR (KBr) 1730, 1591, 1363, 1290, 1249, 1219, 1097, 1002, 929, 884, 800, 720 cm^{-1}.

5-(4-Cyanophenyl)-10,15,20-tris(3,5-di-*tert*-butylphenyl)-porphyrin. 3,5-Di-*tert*-butylbenzaldehyde (16.20 g, 74.20 mmol), 4-cyanobenzaldehyde (3.23 g, 24.6 mmol), and pyrrole (7.30 mL, 105 mmol) were dissolved in dry $CHCl_3$ (2600 mL). The mixture was degassed with nitrogen for 30 min. Then $Et_2O\cdot BF_3$ (4.10 mL, 32.4 mmol) was added to the solution; this mixture was stirred for 2 h under nitrogen atmosphere. Chloranil (18.2 g, 74.0 mmol) was added to the reaction mixture, and this was stirred overnight. The solvent was removed under reduced pressure. Flash column chromatography on silica gel with hexane/benzene (1:1) as an eluent (R_f = 0.25) and subsequent reprecipitation from chloroform/methanol gave desired compound as a dark red solid (3.79 g, 3.88 mmol, 16%). mp > 300 °C; ^{1}H NMR (270 MHz, $CDCl_3$) δ 8.92 (d, J = 5 Hz, 2H), 8.91 (s, 4H), 8.72 (d, J = 5 Hz, 2H), 8.36 (d, J = 8 Hz, 2H), 8.08 (d, J = 2 Hz, 4H), 8.07 (d, J = 2 Hz, 2H), 8.06 (d, J = 8 Hz, 2H), 7.80 (t, J = 2 Hz, 2H), 7.79 (t, J = 2 Hz, 1H), 2.72 (s, 3H), 1.52 (s, 54H), −2.72 (br.s, 2H); MS (FAB) 976 (M + H$^+$); FTIR (KBr) 3732, 1593, 1475, 1394, 1362, 1246, 970, 916, 882, 860, 804, 730, 715, 668 cm^{-1}.

1b. This compound was synthesized from 5-(4-cyanophenyl)-10,15,20-tris(3,5-di-*tert*-butylphenyl)porphyrin by the same method as that described for **3a**. **1b** was obtained as a black red solid from chloroform/methanol (61% yield); mp > 300 °C; ^{1}H NMR (270 MHz, $CDCl_3$) δ 8.93 (d, J = 5 Hz, 2H), 8.88 (s, 4H), 8.87 (d, J = 5 Hz, 2H), 8.08 (d, J = 2 Hz, 4H), 8.07 (d, J = 2 Hz, 2H), 8.01 (d, J = 8 Hz, 2H), 7.78 (t, J = 2 Hz, 2H), 7.77 (t, J = 2 Hz, 1H), 7.07 (d, J = 8 Hz, 2H), 4.22 (s, 2H), 1.60 (s, 2H), 1.54 (s, 54H), −2.71 (br.s, 2H); MS(FAB) 980 (M + H$^+$); FTIR (KBr) 3746, 1695, 1476, 1394, 1366, 1247, 973, 917, 883, 803, 733, 715, 668 cm^{-1}.

4c: Aminomethylporphyrin **1b** (295.7 mg, 0.302 mmol), pyromellitic dianhydride **2** (135 mg, 0.619 mmol), and **3b** (195 mg, 0.940 mmol) in dry DMF (45 mL) were heated at reflux under an atmospheric pressure of nitrogen in the dark for 5 h. The reaction mixture was allowed to cool to room temperature and then evaporated to dryness at a reduced pressure. TLC showed several porphyrin bands (benzene), and the fourth band (R_f = 0.50, benzene/ethyl acetate (15:1)) was separated by flash column chromatography. The fraction was concentrated and dissolved in a mixture of chloroform (53 mL), trifluoroacetic acid (21 mL), and 5% aqueous sulfuric acid (16 mL). After stirring for 16 h, the mixture was poured into 100 mL of water and extracted with $CHCl_3$. The organic layer was washed with saturated $NaHCO_3$ aqueous solution, dried over anhydrous Na_2SO_4, and evaporated. Flash column chromatography on silica gel with chloroform as an eluent (R_f = 0.10, benzene/ethyl acetate (30:1)) and subsequent reprecipitation from chloroform/methanol gave **4c** as a black red solid (50.4 mg, 0.0393 mmol, 13%). mp > 300 °C; ^{1}H NMR (270 MHz, $CDCl_3$) δ 10.09 (s, 1H), 8.88 (s, 4H), 8.85 (d, J = 5 Hz, 2H), 8.77 (d, J = 5 Hz, 2H), 8.30 (s, 2H), 8.22 (d, J = 8 Hz, 2H), 8.08 (s, 4H), 8.07 (s, 2H), 8.05 (d, J = 8 Hz, 2H), 7.83 (d, J = 8 Hz, 2H), 7.78 (s, 3H), 7.71 (d, J = 8 Hz, 2H), 5.24 (s, 2H), 1.55 (s, 54H), −2.79 (br.s, 2H); MS(FAB) 1284 (M + H$^+$); FTIR (KBr) 3742, 1730, 1593, 1508, 1475, 1425, 1364, 1247, 1205 1092, 1000, 972, 915, 883, 802, 724 cm^{-1}.

ZnP-CH$_2$-Im-C$_{60}$. C_{60} (145.6 mg, 0.202 mmol), **4c** (85.8 mg, 0.0668 mmol), and *N*-methylglycine (179 mg, 2.01 mmol) in dry toluene (20 mL) were heated at reflux under an atmospheric pressure of nitrogen in the dark for 10 h. The reaction mixture was allowed to cool to room temperature and then evaporated to dryness at a reduced pressure. Flash column chromatography on silica gel with chloroform as an eluent (R_f = 0.10, chloroform) and subsequent reprecipitation from chloroform/methanol gave the desired product as a dark yellowish brown solid (66.1 mg, 0.0325 mmol, 49%). mp > 300 °C; ^{1}H NMR (270 MHz, $CDCl_3$) δ 8.88 (s, 4H), 8.84 (d, J = 5 Hz, 2H), 8.76 (d, J = 5 Hz, 2H), 8.37 (s, 2H), 8.20 (d, J = 8 Hz, 2H), 8.07 (d, J = 2 Hz, 2H), 8.06 (d, J = 2 Hz, 4H), 7.86 (br.s, 2H), 7.81 (d, J = 8 Hz, 2H), 7.77 (t, J = 2 Hz, 2H), 7.76 (t, J = 2 Hz, 1H), 7.57 (d, J = 8 Hz, 2H), 5.22 (s, 2H), 4.82 (d, J = 10 Hz, 2H), 4.80 (s, 1H), 4.07 (d, J = 10 Hz, 1H), 2.78 (s, 3H), 1.50 (s, 54H), −2.77 (br.s, 2H); MS (MALDI−TOF) 2026 (M + H$^+$); FTIR (KBr) 3735, 1592, 1459, 1363, 1095, 800, 725, 527 cm^{-1}. A saturated methanol solution of $Zn(OAc)_2$ (3 mL) was added to a solution of the sample of the C_{60} adduct (66.1 mg, 0.0325 mmol) in $CHCl_3$ (180 mL) and heated at reflux for 30 min. After cooling, the reaction mixture was washed with water twice and dried over anhydrous Na_2SO_4, and then the solvent was evaporated. Flash column chromatography on silica gel with $CHCl_3$ as an eluent (R_f = 0.45, benzene/ethyl acetate (19:1)) and subsequent reprecipitation from chloroform-methanol gave **ZnP-Im-CH$_2$-C$_{60}$** as a dark brownish violet solid (85% yield, 57.8 mg, 0.0276 mmol). mp > 300 °C; ^{1}H NMR (270 MHz, $CDCl_3$) δ 8.98 (s, 4H), 8.94 (d, J = 5 Hz, 2H), 8.87 (d, J = 5 Hz, 2H), 8.43 (s, 2H), 8.20 (d, J = 8 Hz, 2H), 8.06 (s, 6H), 7.81 (d, J = 8 Hz, 4H), 7.77 (s, 3H), 7.57 (d, J = 8 Hz, 2H), 5.23 (s, 2H), 4.70 (d, J = 10 Hz, 1H), 4.69 (s, 1H), 3.94 (d, J = 10 Hz, 1H), 2.76 (s, 3H), 1.53 (s, 54H); MS (MALDI−TOF) 2095 (M + H$^+$); FTIR (KBr) 1730, 1592, 1475, 1363, 1092, 1002, 797, 718, 527 cm^{-1}.

ZnP-CH$_2$-Im-ref. Aminomethylporphyrin **1b** (302 mg, 0.308 mmol), pyromellitic dianhydride **2** (135 mg, 0.618 mmol), and 4-hexadecylaniline (223 mg, 0.703 mmol) in dry DMF (46 mL) were heated at reflux under an atmospheric pressure of nitrogen in the dark for 11 h. The reaction mixture was allowed to cool to room temperature and then evaporated to dryness at a reduced pressure. TLC showed three porphyrin bands (R_f = 0.65, 0.30, and 0.05, benzene), and the second band was separated by flash column chromatography. Reprecipitation from benzene-acetonitrile gave the desired product as a dark grayish purple solid (176 mg, 0.119 mmol, 39%). mp > 300 °C; ^{1}H NMR (270 MHz, $CDCl_3$) δ 8.88 (s, 4H), 8.84 (d, J = 5 Hz, 2H), 8.78 (d, J = 5 Hz, 2H), 8.37 (s, 2H), 8.21 (d, J = 8 Hz, 2H), 8.07 (s, 6H), 7.81 (d, J = 8 Hz, 2H), 7.79 (s, 3H), 7.35 (s, 2H), 5.23 (s, 2H), 2.67 (t, J = 8 Hz, 2H), 1.7−1.2 (m, 28H), 1.54 (m, 54H), 0.89 (t, J = 8 Hz, 3H), −2.75 (br.s, 2H); MS (FAB) 1480 (M + H$^+$); FTIR (KBr) 3745, 1729, 1593, 1515, 1476, 1362, 1247,

1098, 973, 915, 883, 803, 724 cm^{-1}. A saturated methanol solution of $Zn(OAc)_2$ (3 mL) was added to a solution of the sample of the dyad (176 mg, 0.119 mmol) in $CHCl_3$ (200 mL) and heated at reflux for 30 min. After cooling, the reaction mixture was washed with water twice and dried over anhydrous Na_2SO_4, and then the solvent was evaporated. Flash column chromatography on silica gel with $CHCl_3$ as an eluent (R_f = 0.35, benzene) and subsequent reprecipitation from chloroform/methanol gave **ZnP-Im-CH_2-ref** as a dark grayish solid (90% yield, 165 mg, 0.107 mmol). mp > 300 °C; ^{1}H NMR (270 MHz, $CDCl_3$) δ 9.00 (s, 4H), 8.96 (d, J = 5 Hz, 2H), 8.88 (d, J = 5 Hz, 2H), 8.40 (s, 2H), 8.21 (d, J = 8 Hz, 2H), 8.08 (s, 6H), 7.79 (d, J = 8 Hz, 2H), 7.78 (s, 3H), 7.36 (d, J = 8 Hz, 2H), 7.34 (d, J = 8 Hz, 2H), 5.23 (s, 2H), 2.68 (t, J = 8 Hz, 2H), 1.7−1.2 (m, 28H), 1.51 (s, 54H), 0.88 (t, J = 8 Hz, 3H); MS (FAB) 1542 ($M + H^+$); FTIR (KBr) 1730, 1591, 1363, 1290, 1249, 1219, 1097, 1002, 929, 884, 800, 724 cm^{-1}.

ZnP-CH_2-ref. To a stirred solution of **1b** (101 mg, 0.103 mmol) in dry CH_2Cl_2 (10 mL) was added acetic anhydride (0.040 mL, 0.420 mmol) dropwise at 0 °C, and stirring was continued at 0 °C for 20 min. The reaction mixture was allowed to cool to room temperature and then evaporated to dryness at a reduced pressure. Flash column chromatography on silica gel with toluene/ethyl acetate (1:1) as an eluent (R_f = 0.35) and subsequent reprecipitation from benzene/acetonitrile gave the desired product as a dark grayish brown solid (80.7 mg, 0.0789 mmol, 77%). mp > 300 °C; ^{1}H NMR (270 MHz, $CDCl_3$) δ 8.89 (s, 4H), 8.88 (d, J = 5 Hz, 2H), 8.81 (d, J = 5 Hz, 2H), 8.20 (d, J = 8 Hz, 2H), 8.08 (s, 6H), 7.79 (s, 3H), 6.02 (t, J = 8 Hz, 1H), 4.78 (d, J = 8 Hz, 2H), 2.18 (s, 3H), 1.52 (s, 54H), −2.71 (br.s, 2H); MS (FAB) 1022 ($M + H^+$); IR (KBr) 1260, 1096, 1015, 922, 795, 706 cm^{-1}. A saturated methanol solution of $Zn(OAc)_2$ (3 mL) was added to a solution of the sample of the porphyrin (80.7 mg, 0.0789 mmol) in $CHCl_3$ (200 mL) and heated at reflux for 30 min. After cooling, the reaction mixture was washed with water twice and dried over anhydrous Na_2SO_4, and then the solvent was evaporated. Flash column chromatography on silica gel with $CHCl_3$ as an eluent (R_f = 0.35, benzene) and subsequent reprecipitation from benzene-acetonitrile gave **Zn-CH_2-ref** as a deep purple solid (81% yield, 69.3 mg, 0.0639 mmol). mp > 300 °C; ^{1}H NMR (270 MHz, $CDCl_3$) δ 9.00 (s, 4H), 8.99 (d, J = 5 Hz, 2H), 8.91 (d, J = 5 Hz, 2H), 8.20 (d, J = 8 Hz, 2H), 8.09 (d, J = 2 Hz, 4H), 8.08 (d, J = 2 Hz, 2H), 7.79 (t, J = 2 Hz, 2H), 7.78 (t, J = 2 Hz, 1), 6.00 (t, J = 8 Hz, 1H), 4.74 (d, J = 8 Hz, 2H), 2.13 (s, 3H), 1.52 (s, 54H); MS (FAB) 1085 ($M + H^+$); IR (KBr) 1247, 1217, 1001, 947, 930, 880, 823, 797, 716 cm^{-1}.

Spectral Measurements. Time-resolved fluorescence spectra of the porphyrin moiety of the dyads and triads were measured by a single-photon counting method using a second harmonic generation (SHG, 524 nm) of a semiconductor YLF laser (Lightwave 131-1047-300, fwhm = 20 ps) as an excitation source.

Picosecond transient absorption spectra were measured by means of a picosecond dye laser (fwhm 12 ps) pumped by the second harmonic of a repetitive mode-locked Nd^{3+}:YAG laser (Quantel, Picochrome YG-503 C/PTL-10).[23b] The 590 nm output of the dye laser (Rhodamine 6G) was used for excitation.

Nanosecond transient absorption measurements were carried out using SHG (550 nm) of Nd:YAG laser (Spectra-Physics, Quanta-Ray GCR-130, fwhm 6 ns) as an excitation source. For transient absorption spectra in the near-IR region (600−1600 nm), monitoring light from a pulsed Xe lamp was detected with a Ge-avalanche photodiode (Hamamatsu Photonics, B2834). Details of the transient absorption measurements were described elsewhere.[23f] All of the samples (10^{-4}∼10^{-5} M) in a quartz cell (1 × 1 cm) were deaerated by bubbling argon through the solution for 15 min.

Electrochemical Measurements. The differential pulse voltammetry (DPV) measurements of the dyads and triads were performed on a BAS 50W electrochemical analyzer in a deaerated CH_2Cl_2 solution containing 0.10 M n-Bu_4NPF_6 as a supporting electrolyte at a sweep rate of 10 mV s^{-1} at 298 K (see Supporting Information, S3). The glassy carbon working electrode was polished with BAS polishing alumina suspension and rinsed with acetone before use. The counter electrode was a platinum wire. The measured potentials were recorded with respect to an Ag/AgCl (saturated KCl) reference electrode. Ferrocene/ferricenium was used as an external standard.

Acknowledgment. This work was supported by COE, Grant-in-Aid for Scientific Research, Specially Promoted Research (No. 10102007), and the Development of Innovative Technology (No.12310) from the Ministry of Education, Culture, Sports, Science and Technology of Japan.

Supporting Information Available: Kinetic analysis of the time profile of transient absorption (S1,S2), DPV voltammogram of **ZnP-CH_2-Im-C_{60}** (S3), differential absorption spectra obtained upon *picosecond* flash photolysis of **ZnP-Im-CH_2-C_{60}** in 1,4-dioxane (S4), time-profile of transient absorbance of **ZnP-Im-CH_2-C_{60}** in 1,4-dioxane (S5), differential absorption spectra obtained upon *nanosecond* flash photolysis of **ZnP-Im-CH_2-C_{60}** in 1,4-dioxane (S6; 6 page, print/PDF). This material is available free of charge via the Internet at http://pubs.acs.org.

References and Notes

(1) (a) Bixon, M.; Jortner, J. *Adv. Chem. Phys.* **1999**, *106*, 35. (b) Skourtis, S. S.; Beratan, D. N. *Adv. Chem. Phys.* **1999**, *106*, 377. (c) Iversen, G.; Kharkats, Y. I.; Kuznetsov, A. M.; Ulstrup, J. *Adv. Chem. Phys.* **1999**, *106*, 453. (d) Newton, M. D. In *Electron Transfer in Chemistry*; Balzani, V., Ed.; Wiley-VCH: Weinheim, Germany, 2001; Vol. 1, pp 3−63. (e) Paddon-Row: M. N. In *Electron Transfer in Chemistry*; Balzani, V., Ed.; Wiley-VCH: Weinheim, Germany, 2001; Vol. 3, pp 179−271.

(2) The function of the intermediary bacteriochlorophyll (BChl), located between bacteriochlorophyll dimer (P) and bacteriopheophytin (Bphe) in the bacterial photosynthetic reaction center, has been a controversial issue of whether stepwise ET occurs from $^1P^*$ to Bphe via BChl or whether BChl participates virtually via a superexchange mechanism.[1,3]

(3) (a) *Anoxygenic Photosynthetic Bacteria*; Blankenship, R. E., Madigan, M. T., Bauer, C. E., Eds.; Kluwer Academic Publishers: Dordecht, The Netherlands, 1995. (b) *The Photosynthetic Reaction Center*; Deisenhofer, J., Norris, J. R., Eds.; Academic Press: San Diego, CA, 1993.

(4) Bixon, M.; Jortner, J.; Michel-Beyerle, M. E. *Biochim. Biophys. Acta* **1991**, *1056*, 301.

(5) (a) Sessler, J. L.; Johnson, M. R.; Lin, T.-Y. *Tetrahedron* **1989**, *45*, 4767. (b) Sessler, J. L.; Johnson, M. R.; Creager, S. E.; Fettinger, J. C.; Ibers, J. A. *J. Am. Chem. Soc.* **1990**, *112*, 9310. (c) Rodriguez, J.; Kirmaier, C.; Johnson, M. R.; Friesner, R. A.; Holten, D.; Sessler, J. L. *J. Am. Chem. Soc.* **1991**, *113*, 1652.

(6) (a) Wasielewski, M. R.; Niemczyk, M. P.; Johnson, D. G.; Svec, W. A.; Minsek, D. W. *Tetrahedron* **1989**, *45*, 4785. (b) Johnson, D. G.; Niemczyk, M. P.; Minsek, D. W.; Wiederrecht, G. P.; Svec, W. A.; Gaines, G. L., III.; Wasielewski, M. R. *J. Am. Chem. Soc.* **1993**, *115*, 5692. (c) Miller, S. E.; Lukas, A. S.; Marsh, E.; Bushard, P.; Wasielewski, M. R. *J. Am. Chem. Soc.* **2000**, *122*, 7802. (d) Gosztola, D.; Wang, B.; Wasielewski, M. R. *J. Photochem. Photobiol. A* **1996**, *102*, 71.

(7) (a) Andersson, M.; Linke, M.; Chambron, J.-C.; Davidsson, J.; Heitz, V.; Sauvage, J.-P.; Hammarstroem, L. *J. Am. Chem. Soc.* **2000**, *122*, 3526. (b) Chambron, J. C.; Harriman, A.; Heitz, V.; Sauvage, J. P. *J. Am. Chem. Soc.* **1993**, *115*, 7419. (c) Brun, A. M.; Atherton, S. J.; Harriman, A.; Heitz, V.; Sauvage, J. P. *J. Am. Chem. Soc.* **1992**, *114*, 4632. (d) Chambron, J. C.; Collin, J. P.; Dalbavie, J. O.; Dietrich-Buchecker, C. O.; Heitz, V.; Odobel, F.; Solladie, N.; Sauvage, J. P. *Coord. Chem. Rev.* **1998**, *180*, 1299. (e) Harriman, A.; Sauvage, J. P. *Chem. Soc. Rev.* **1996**, *25*, 41. (f) Harriman, A.; Heitz, V.; Sauvage, J. P. *J. Phys. Chem.* **1993**, *97*, 5940.

(8) (a) Osuka, A.; Marumo, S.; Mataga, N.; Taniguchi, S.; Okada, T.; Yamazaki, I.; Nishimura, Y.; Ohno, T.; Nozaki, K. *J. Am. Chem. Soc.* **1996**, *118*, 155. (b) Osuka, A.; Mataga, N.; Okada, T. *Pure Appl. Chem.* **1997**, *69*, 797. (c) Osuka, A.; Yamada, H.; Maruyama, K.; Mataga, N.; Asahi, T.; Ohkouchi, M.; Okada, T.; Yamazaki, I.; Nishimura, Y. *J. Am. Chem. Soc.* **1993**, *115*, 9439. (d) Osuka, A.; Yamada, H.; Shinoda, S.; Nozaki, K.; Ohno, T. *Chem. Phys. Lett.* **1995**, *238*, 37.

(9) (a) Kaplan, R. W.; Napper, A. M.; Waldeck, D. H.; Zimmt, M. B. *J. Am. Chem. Soc.* **2000**, *122*, 12039. (b) Read, I.; Napper, A.; Kaplan, R.; Zimmt, M. B.; Waldeck, D. H. *J. Am. Chem. Soc.* **1999**, *121*, 10976. (c) Han, H.; Zimmt, M. B. *J. Am. Chem. Soc.* **1998**, *120*, 8001. (d) Kumar, K.; Lin, Z.; Waldeck, D. H.; Zimmt, M. B. *J. Am. Chem. Soc.* **1996**, *118*, 243. (e) Read, I.; Napper, A.; Zimmt, M. B.; Waldeck, D. H. *J. Phys. Chem. A* **2000**, *104*, 9385.

(10) (a) Roest, M. R.; Lawson, J. M.; Paddon-Row, M. N.; Verhoeven, J. W. *Chem. Phys. Lett.* **1994**, *230*, 536. (b) Willemse, R. J.; Piet, J. J.; Warman, J. M.; Hartl, F.; Verhoeven, J. W.; Brouwer, A. M. *J. Am. Chem. Soc.* **2000**, *122*, 3721. (c) Lokan, N. R.; Paddon-Row, M. N.; Koeberg, M.; Verhoeven, J. W. *J. Am. Chem. Soc.* **2000**, *122*, 5075. (d) Jolliffe, K. A.; Bell, T. D. M.; Ghiggino, K. P.; Langford, S. J.; Paddon-Row, M. N. *Angew. Chem. Int. Ed.* **1998**, *37*, 916. (e) Verhoeven, J. W. *Adv. Chem. Phys.* **1999**, *106*, 603.

(11) Kuciauskas, D.; Liddell, P. A.; Hung, S.-C.; Lin, S.; Stone, S.; Seely, G. R.; Moore, A. L.; Moore, T. A.; Gust, D. *J. Phys. Chem. B* **1997**, *101*, 429.

(12) (a) Pollinger, F.; Heitele, H.; Michel-Beyerle, M. E.; Tercel, M.; Staab, H. A. *Chem. Phys. Lett.* **1993**, *209*, 251. (b) Elliott, C. M.; Derr, D. L.; Ferrere, S.; Newton, M. D.; Liu, Y. P. *J. Am. Chem. Soc.* **1996**, *118*, 5221. (c) Kilså, K.; Kajanus, J.; Macpherson, A. N.; Mårtensson, J.; Albinsson, B. *J. Am. Chem. Soc.* **2001**, *123*, 3069.

(13) (a) Lewis, F. D.; Wu, T. F.; Liu, X. Y.; Letsinger, R. L.; Greenfield, S. R.; Miller, S. E.; Wasielewski, M. R. *J. Am. Chem. Soc.* **2000**, *122*, 2889. (b) Lewis, F. D.; Liu, X. Y.; Liu, J. Q.; Miller, S. E.; Hayes, R. T.; Wasielewski, M. R. *Nature* **2000**, *406*, 51. (c) Lewis, F. D.; Kalgutkar, R. S.; Wu, Y.; Liu, X.; Liu, J.; Hayes, R. T.; Miller, S. E.; Wasielewski, M. R. *J. Am. Chem. Soc.* **2000**, *122*, 12346. (d) Lewis, F. D.; Letsinger, R. L.; Wasielewski, M. R. *Acc. Chem. Res.* **2001**, *34*, 159. (e) Page, C. C.; Moser, C. C.; Chen, X. X.; Dutton, P. L. *Nature* **1999**, *402*, 47. (f) Meggers, E.; Michel-Beyerle, M. E.; Giese, B. *J. Am. Chem. Soc.* **1998**, *120*, 12950. (g) Arkin, M. R.; Stemp, E. D. A.; Holmlin, R. E.; Barton, J. K.; Hörmann, A.; Olson, E. J. C.; Barabara, P. F. *Science*, **1996**, *273*, 475.

(14) (a) Tsue, H.; Imahori, H.; Kaneda, T.; Tanaka, Y.; Okada, T.; Tamaki, K.; Sakata, Y. *J. Am. Chem. Soc.* **2000**, *122*, 2279.

(15) Imahori, H.; Yamada, K.; Hasegawa, M.; Taniguchi, S.; Okada, T.; Sakata, Y. *Angew. Chem. Int. Ed.* **1997**, *36*, 2626.

(16) (a) Martín, N.; Sánchez, L.; Illescas, B.; Pérez, I. *Chem. Rev.* **1998**, *98*, 2527. (b) Prato, M. *J. Mater. Chem.* **1997**, *7*, 1097. (c) Diederich, F.; Gómez-López, M. *Chem. Soc. Rev.* **1999**, *28*, 263. (d) Guldi, D. M.; Kamat, P. V. In *Fullerenes*; Kadish, K. M., Ruoff, R. S., Eds.; John Wiley & Sons: New York, 2000; Chapter 5, pp 225−281. (e) Fukuzumi, S.; Guldi, D. M. In *Electron Transfer in Chemistry*; Balzani, V., Ed.; Wiley-VCH: Weinheim, Germany, 2001; Vol. 2, pp 270−337.

(17) (a) Liddell, P. A.; Sumida, J. P.; Macpherson, A. N.; Noss, L.; Seely, G. R.; Clark, K. N.; Moore, A. L.; Moore, T. A.; Gust, D. *Photochem. Photobiol.* **1994**, *60*, 537. (b) Kuciauskas, D.; Lin, S.; Seely, G. R.; Moore, A. L.; Moore, T. A.; Gust, D.; Drovetskaya, T.; Reed, C. A.; Boyd, P. D. W. *J. Phys. Chem.* **1996**, *100*, 15926. (c) Liddell, P. A.; Kuciauskas, D.; Sumida, J. P.; Nash, B.; Nguyen, D.; Moore, A. L.; Moore, T. A.; Gust, D. *J. Am. Chem. Soc.* **1997**, *119*, 1400. (d) Kuciauskas, D.; Liddell, P. A.; Lin, S.; Johnson, T. E.; Weghorn, S. J.; Lindsey, J. S.; Moore, A. L.; Moore, T. A.; Gust, D. *J. Am. Chem. Soc.* **1999**, *121*, 8604. (e) Kuciauskas, D.; Liddell, P. A.; Lin, S.; Stone, S. G.; Moore, A. L.; Moore, T. A.; Gust, D. *J. Phys. Chem. B* **2000**, *104*, 4307.

(18) (a) Williams, R. M.; Zwier, J. M.; Verhoeven, J. W. *J. Am. Chem. Soc.* **1995**, *117*, 4093. (b) Lawson, J. M.; Oliver, A. M.; Rothenfluh, D. F.; An, Y.-Z.; Ellis, G. A.; Ranasinghe, M. G.; Khan, S. I.; Franz, A. G.; Ganapathi, P. S.; Shephard, M. J.; Paddon-Row, M. N.; Rubin, Y. *J. Org. Chem.* **1996**, *61*, 5032. (c) Williams, R. M.; Koeberg, M.; Lawson, J. M.; An, Y.-Z.; Rubin, Y.; Paddon-Row, M. N.; Verhoeven, J. W. *J. Org. Chem.* **1996**, *61*, 5055. (d) Bell, T. D. M.; Smith, T. A.; Ghiggino, K. P.; Ranasinghe, M. G.; Shephard, M. J.; Paddon-Row, M. N. *Chem. Phys. Lett.* **1997**, *268*, 223.

(19) (a) Jensen, A. W.; Wilson, S. R.; Schuster, D. I. *Bioorg. Med. Chem.* **1996**, *4*, 767. (b) Baran, P. S.; Monaco, R. R.; Khan, A. U.; Schuster, D. I.; Wilson, S. R. *J. Am. Chem. Soc.* **1997**, *119*, 8363. (c) Schuster, D. I.; Cheng, P.; Wilson, S. R.; Prokhorenko, V.; Katterle, M.; Holzwarth, A. R.; Braslavsky, S. E.; Klihm, G.; Williams, R. M.; Luo, C. *J. Am. Chem. Soc.* **1999**, *121*, 11599. (d) Fong, R., II.; Schuster, D. I.; Wilson, S. R. *Org. Lett.* **1999**, *1*, 729. (e) Sun, Y.; Wilson, S. R.; Schuster, D. I. *J. Am. Chem. Soc.* **2001**, *123*, 5348.

(20) (a) Armaroli, N.; Diederlich, F.; Dietrich-Buchecker, C. O.; Flamigni, L.; Marconi, G.; Nierengarten, J.-F.; Sauvage, J.-P. *Chem. Eur. J.* **1998**, *4*, 406. (b) Armspach, D.; Constable, E. C.; Diederlich, F.; Housecroft, C. E.; Nierengarten, J.-F. *Chem. Eur. J.* **1998**, *4*, 723. (c) Armaroli, N.; Marconi, G.; Echegoyen, L.; Bourgeois, J.-P.; Diederlich, F. *Chem. Eur. J.* **2000**, *6*, 1629. (d) van Hal, P. A.; Knol, J.; Langeveld-Voss, B. M. W.; Meskers, S. C. J.; Hummelen, J. C.; Janssen, R. A. J. *J. Phys. Chem. A* **2000**, *104*, 5974. (e) Eckert, J.-F.; Nicoud, J.-F.; Nierengarten, J.-F.; Liu, S.-G.; Echegoyen, L.; Barigelletti, F.; Armaroli, N.; Ouali, L.; Krasnikov, V.; Hadziioannou, G. *J. Am. Chem. Soc.* **2000**, *122*, 7467.

(21) (a) Kamat, P. V.; Barazzouk, S.; Hotchandani, S.; Thomas, K. G. *Chem. Eur. J.* **2000**, *6*, 3914. (b) Thomas, K. G.; Biju, V.; Guldi, D. M.; Kamat, P. V.; George, M. V. *J. Phys. Chem. B* **1999**, *103*, 8864. (c) Thomas, K. G.; Biju, V.; Guldi, D. M.; Kamat, P. V.; George, M. V. *J. Phys. Chem. A* **1999**, *103*, 10755. (d) Tkachenko, N. V.; Rantala, L.; Tauber, A. Y.; Helaja, J.; Hynninen, P. H.; Lemmetyinen, H. *J. Am. Chem. Soc.* **1999**, *121*, 9378. (e) Tkachenko, N. V.; Vuorimaa, E.; Kesti, T.; Alekseev, A. S.; Tauber, A. Y.; Hynninen, P. H.; Lemmetyinen, H. *J. Phys. Chem. B* **2000**, *104*, 6371. (f) D'Souza, F.; Deviprasad, G. R.; El-Khouly, M. E.; Fujitsuka, M.; Ito, O. *J. Am. Chem. Soc.* **2001**, *123*, 5277.

(22) (a) Guldi, D. M.; Maggini, M.; Scorrano, G.; Prato, M. *J. Am. Chem. Soc.* **1997**, *119*, 974. (b) Maggini, M.; Guldi, D. M.; Mondini, S.; Scorrano, G.; Paolucci. F.; Ceroni, P.; Roffia, S. *Chem. Eur. J.* **1998**, *4*, 1992. (c) Polese, A.; Mondini, S.; Bianco, A.; Toniolo, C.; Scorrano, G.; Guldi, D. M.; Maggini, M. *J. Am. Chem. Soc.* **1999**, *121*, 3446. (d) Guldi, D. M.; Maggini, M.; Menna, E.; Scorrano, G.; Ceroni, P.; Marcaccio, M.; Paolucci, F.; Roffia, S. *Chem. Eur. J.* **2001**, *7*, 1597. (e) Da Ros, T.; Prato, M.; Guldi, D. M.; Ruzzi, M.; Pasimeni, L. *Chem. Eur. J.* **2001**, *7*, 816.

(23) (a) Imahori, H.; Hagiwara, K.; Akiyama, T.; Taniguchi, S.; Okada, T.; Sakata, Y. *Chem. Lett.* **1995**, 265. (b) Imahori, H.; Hagiwara, K.; Aoki, M.; Akiyama, T.; Taniguchi, S.; Okada, T.; Shirakawa, M.; Sakata, Y. *J. Am. Chem. Soc.* **1996**, *118*, 11771. (c) Sakata, Y.; Imahori, H.; Tsue, H.; Higashida, S.; Akiyama, T.; Yoshizawa, E.; Aoki, M.; Yamada, K.; Hagiwara, K.; Taniguchi, S.; Okada, T. *Pure Appl. Chem.* **1997**, *69*, 1951. (d) Tamaki, K.; Imahori, H.; Nishimura, Y.; Yamazaki, I.; Shimomura, A.; Okada, T.; Sakata, Y. *Chem. Lett.* **1999**, 227. (e) Yamada, K.; Imahori, H.; Nishimura, Y.; Yamazaki, I.; Sakata, Y. *Chem. Lett.* **1999**, 895. (f) Imahori, H.; El-Khouly, M. E.; Fujitsuka, M.; Ito, O.; Sakata, Y.; Fukuzumi, S. *J. Phys. Chem. A* **2001**, *105*, 325.

(24) (a) Tamaki, K.; Imahori, H.; Nishimura, Y.; Yamazaki, I.; Sakata, Y. *Chem. Commun.* **1999**, 625. (b) Luo, C.; Guldi, D. M.; Imahori, H.; Tamaki, K.; Sakata, Y. *J. Am. Chem. Soc.* **2000**, *122*, 6535. (c) Imahori, H.; Tamaki, K.; Guldi, D. M.; Luo, C.; Fujitsuka, M.; Ito, O.; Sakata, Y.; Fukuzumi, S. *J. Am. Chem. Soc.* **2001**, *123*, 2607. (d) Fukuzumi, S.; Imahori, H.; Yamada, H.; El-Khouly, M. E.; Fujitsuka, M.; Ito, O.; Guldi, D. M. *J. Am. Chem. Soc.* **2001**, *123*, 2571. (e) Imahori, H.; Guldi, D. M.; Tamaki, K.; Yoshida, H.; Luo, C.; Sakata, Y.; Fukuzumi, S. *J. Am. Chem. Soc.* **2001**, *123*, 6617. (f) Fukuzumi, S.; Ohkubo, K.; Imahori, H.; Shao, J.; Ou, Z.; Zheng, G.; Chen, Y.; Pandey, R. K.; Fujitsuka, M.; Ito, O.; Kadish, K. M. *J. Am. Chem. Soc.* **2001**, *123*, 10676. (g) Fukuzumi, S.; Imahori, H.; Okamoto, K.; Yamada, H.; Fujitsuka, M.; Ito, O.; Guldi, D. M. *J. Phys. Chem. A* in press.

(25) (a) Imahori, H.; Ozawa, S.; Ushida, K.; Takahashi, M.; Azuma, T.; Ajavakom, A.; Akiyama, T.; Hasegawa, M.; Taniguchi, S.; Okada, T.; Sakata, Y. *Bull. Chem. Soc. Jpn.* **1999**, *72*, 485. (b) Imahori, H.; Yamada, H.; Nishimura, Y.; Yamazaki, I.; Sakata, Y. *J. Phys. Chem. B* **2000**, *104*, 2099. (c) Imahori, H.; Norieda, H.; Yamada, H.; Nishimura, Y.; Yamazaki, I.; Sakata, Y.; Fukuzumi, S. *J. Am. Chem. Soc.* **2001**, *123*, 100. (d) Fukuzumi, S.; Imahori, H. In *Electron Transfer in Chemistry*; Balzani, V., Ed.; Wiley-VCH: Weinheim, Germany, 2001; Vol. 2, pp 927−975 (e) Imahori, H.; Fukuzumi, S. *Adv. Mater.* **2001**, *13*, 1197. (f) Imahori, H.; Hasobe, T.; Yamada, H.; Kamat, P. V.; Barazzouk, S.; Fujitsuka, M.; Ito, O.; Fukuzumi, S. *Chem. Lett.* **2001**, 784.

(26) (a) Imahori, H.; Sakata, Y. *Adv. Mater.* **1997**, *9*, 537. (b) Imahori, H.; Sakata, Y. *Eur. J. Org. Chem.* **1999**, 2445. (c) Guldi, D. M. *Chem. Commun.* **2000**, 321. (d) Guldi, D. M.; Prato, M. *Acc. Chem. Res.* **2000**, *33*, 695.

(27) (a) Imahori, H.; Hagiwara, K.; Akiyama, T.; Aoki, M.; Taniguchi, S.; Okada, T.; Shirakawa, M.; Sakata, Y. *Chem. Phys. Lett.* **1996**, *263*, 545. (b) Tkachenko, N. V.; Guenther, C.; Imahori, H.; Tamaki, K.; Sakata, Y.; Fukuzumi, S.; Lemmetyinen, H. *Chem. Phys. Lett.* **2000**, *326*, 344. (c) Imahori, H.; Tamaki, K.; Yamada, H.; Yamada, K.; Sakata, Y.; Nishimura, Y.; Yamazaki, I.; Fujitsuka, M.; Ito, O. *Carbon* **2000**, *38*, 1599. (d) Imahori, H.; Tkachenko, N. V.; Vehmanen, V.; Tamaki, K.; Lemmetyinen, H.; Sakata, Y.; Fukuzumi, S. *J. Phys. Chem. A* **2001**, *105*, 1750. (e) Vehmanen, V.; Tkachenko, N. V.; Imahori, H.; Fukuzumi, S.; Lemmetyinen, H. *Spectrochim. Acta, Part A* **2001**, *57*, 2229.

(28) Guldi, D. M.; Asmus, K.-D. *J. Am. Chem. Soc.* **1997**, *119*, 5744.

(29) Lindsey, J. S.; Schreiman, I. C.; Hsu, H. C.; Kearney, P. C.; Marguerettaz, A. M. *J. Org. Chem.* **1987**, *52*, 827.

(30) Imahori, H.; Azuma, T.; Ajavakom, A.; Norieda, H.; Yamada, H.; Sakata, Y. *J. Phys. Chem. B* **1999**, *103*, 7233.

(31) Maggini, M.; Scorrano, G.; Prato, M. *J. Am. Chem. Soc.* **1993**, *115*, 9798.

(32) (a) Fuhrhop, J.-H.; Mauzerall, D. *J. Am. Chem. Soc.* **1969**, *91*, 4174. (b) Chosrowjan, H.; Taniguchi, S.; Okada, T.; Takagi, S.; Arai, T.; Tokumaru, K. *Chem. Phys. Lett.* **1995**, *242*, 644.

(33) Ohkohchi, M.; Takahashi, A.; Mataga, N.; Okada, T.; Osuka, A.; Yamada, H.; Maruyama, K. *J. Am. Chem. Soc.* **1993**, *115*, 12137.

(34) Asahi, T.; Ohkohchi, M.; Takahashi, A.; Matsusaka, R.; Mataga, N.; Zhang, R. P.; Osuka, A.; Maruyama, K. *J. Am. Chem. Soc.* **1993**, *115*, 5665.

(35) Tan, Q.; Kuciauskas, D.; Lin, S.; Stone, S.; Moore, A. L.; Moore, T. A.; Gust, D. *J. Phys. Chem. B* **1997**, *101*, 5214.

(36) $-\Delta G^0_{ET}$ values are assumed to be similar in CH_2Cl_2 and THF, because of the ϵ_s values are largely the same in CH_2Cl_2 (8.9) and THF (7.58).

(37) The CR rates of the dyads are larger than the corresponding CS rates in both 1,4-dioxane and THF, except the case of **ZnP-CH$_2$-Im-ref** in 1,4-dioxane. Because the R_{ee} value (6.4 Å) of **ZnP-CH$_2$-Im-ref** is slightly larger than that (5.7 Å) of **ZnP-Im-CH$_2$-ref** and **ZnP-Im-ref**, the charge-separated state of the former in 1,4-dioxane may be destabilized as compared to those of the latter, resulting to the comparable ET rates for CS1 and CR1.

(38) The initial CS rates ($k_{ET(CS1)}$) in the triads without a methylene spacer between the Im and C_{60} moieties (i.e., **ZnP-CH$_2$-Im-C$_{60}$** and **ZnP-Im-C$_{60}$**) are by ~50−110% larger than the CS rates of the corresponding porphyrin-imide dyads, whereas the $k_{ET(CS1)}$ values in the triad with a methylene spacer between the Im and C_{60} moieties are virtually the same as those of the corresponding dyad. Thus, the acceleration effect may result from the electron-withdrawing character of the C_{60} moiety attached to the Im moeity.[15] There is also another possibility that direct ET from ^{1}ZnP* to C_{60} occurs in addition to the sequential ET from ^{1}ZnP* to C_{60} via the Im moiety. The somewhat larger $k_{ET(CS1)}$ values of the triads as compared with the values of dyads without C_{60} (Table 2) may be ascribed to the occurrence of such a direct ET pathway.

(39) The total quantum yield of the CS (0.49) for **ZnP-Im-C$_{60}$** in THF agrees largely with the corresponding value (0.46) obtained by the transient absorption spectrum [ϵ = 13 500 M^{-1} cm^{-1} (ZnP$^{\bullet+}$) at 620 nm].

(40) The CSH rates of **ZnP-CH$_2$-Im-C$_{60}$** in 1,4-dioxane and THF are smaller than those of **ZnP-Im-C$_{60}$**, respectively. Because the R_{cc} value of **ZnP-CH$_2$-Im-C$_{60}$** (11.7 Å) is small as compared to that of **ZnP-Im-C$_{60}$** (12.5 Å), the retardation of CSH in the former may result from the strong Coulombic interaction between an electron in the imide radical anion and a positive charge in the porphyrin radical cation in the former relative to the latter.

(41) *Physical Methods of Chemistry*; Rossiter, B. W., Hamilton, J. F., Eds.; Wiley-International: New York, 1986; Vol IIIB, p 114.

(42) Nojiri, T.; Watanabe, A.; Ito, O. *J. Phys. Chem. A* **1998**, *102*, 5215.

(43) The decay of charge-separated state to porphyrin and C_{60} excited triplet states rather than to the ground state has been reported in porphyrin-fullerene linked systems.[23f] This can be rationalized by the small reorganization energies of ET.[26,27] Namely, on the Marcus parabolic curve, the former ET processes are located near to the top region, whereas the latter process to the ground state is forced to be shifted deeply into the inverted region.

(44) Helms, A.; Heiler, D.; McLendon, G. *J. Am. Chem. Soc.* **1992**, *114*, 6227.

(45) On the basis of Marcus plot for ET processes of **ZnP-C$_{60}$** dyad (λ = 0.66 eV in THF) and **ZnP-H$_2$P-C$_{60}$** triad (λ = 1.09 eV in THF),[24c,e] the λ value in the present systems is estimated to be ~0.9 eV, which is smaller by 0.5−0.6 eV than the driving force for CR2 (1.44−1.46 eV) from $C_{60}^{\bullet-}$ to the ZnP$^{\bullet+}$. This implies that the CR process of **ZnP-Im-C$_{60}$** is located deeply into the inverted region of the Marcus parabola, thus ruling out the possibility of an activation less process near the top region of the Marcus parabola.

(46) The apparent E_a value of **ZnP-CH$_2$-Im-C$_{60}$** (0.07 eV) is smaller than the difference in the energy level between **ZnP$^{\bullet+}$-CH$_2$-Im$^{\bullet-}$-C$_{60}$** and **ZnP$^{\bullet+}$-CH$_2$-Im-C$_{60}^{\bullet-}$** (0.12 eV) probably because of some contribution of the temperature independent process in the examined temperature range.

(47) The two systems (**ZnP-Im-CH$_2$-C$_{60}$** and **ZnP-CH$_2$-Im-C$_{60}$**) that show the temperature dependence have a larger degree of flexibility because of the methylene group. Thus, there is another possibility that different conformations give rise to different temperature dependence. Such a possibility is ruled out at least in the former case, because of no deviation from the straight line for the plot (Figure 7a). In contrast, a conformational change might occur with decreasing the temperature in the latter case, leading to the deviation from the straight line in the plot (Figure 7c). However, such a conformational change is unlikely to occur because all of the decay processes can be analyzed by a single-exponential component at various temperatures.[34]

(48) (a) Kramers, H. A. *Physica* **1934**, *1*, 182. (b) Bixon, M.; Jortner, J.; Michel-Beyerle, M. E.; Ogrodnik, A. *Biochim. Biophys. Acta* **1989**, *977*, 273.